Elsevier Editorial System(tm) for
Environmental and Experimental Botany
Manuscript Draft

Manuscript Number: EEB-D-16-00439R2

Title: SURVIVE OR DIE? A MOLECULAR INSIGHT INTO SALT-DEPENDANT SIGNALING NETWORK

Article Type: Research Paper

Keywords: Antirrhinum majus L., NaCl stress, RNAseq, Transcriptome, ABA, ethylene, snapdragon, Ca2+ signaling, cell cycle progression

Corresponding Author: Dr. Alice trivellini,

Corresponding Author's Institution:

First Author: Alice trivellini

Order of Authors: Alice trivellini; Mariella Lucchesini; Antonio Ferrante; Giulia Carmassi; Guido Scatena; Paolo Vernieri; Anna Mensuali-Sodi

Abstract: The response of plants to salt stress involves dynamic changes in growth and signaling leading to successful adaptation or death. To elucidate how these opposed events are coordinated we identified a salt-tolerant (obesifruticosa) and a salt-sensitive (aestiva) Antirrhinum majus mutants using shoots as sensitive indicator of stress magnitude. A series of physiological tests were performed that compared the response after 6 hours and 3 days of these contrasting mutants grown in agar under a single (200 mM) NaCl concentration, including shoot area, root length, relative water content, plant height, and overall biomass accumulation. Additional measurements of ABA content, chlorophyll degradation, ethylene production, net photosynthesis rates and Na+, K+, Ca2+, and Mg2+ content were also reported. RNA-seq analysis was performed on the two mutants after 6 hours and 3 days under 200 mM NaCl. A total of 9199 transcripts were found to be differentially expressed in response to NaCl treatment in the two mutants. A large collection of known genes, including MAPKs, CDKs, CDPKs, CIPKs, various transcription factors, various ion transport proteins, and various genes involved in ABA and ethylene signaling pathways were described in detail that displayed differential expression profiles. Overall these data provided evidences of a putative osmotic tolerance sensing and signaling mechanism through a better integration and transduction of environmental cues into growth programs. The reprogramming of calcium-signaling components generates specific stress signatures affecting differentially the salinity tolerance traits such as tissue tolerance and anion exclusion. Interestingly, the hormones ABA and ethylene may action as a positive regulators of salt acclimation by the modulation of their signal transduction pathway.

Cover Letter

Dear Editor,

Please find attached a manuscript entitled “SURVIVE OR DIE? A MOLECULAR INSIGHT INTO SALT-DEPENDANT HORMONAL-SIGNALING NETWORK”, by Alice Trivellini, Lucchesini Mariella, Antonio Ferrante, Giulia Carmassi, Guido Scatena, Paolo Vernieri, Anna Mensuali-Sodi, that we submit for consideration for publication in Environmental and Experimental Botany.

By classic physiological experiments coupled with RNA-Seq data, we propose an original experimental approach to identified specific signatures in salt stress, analyzing two distinct modes, acclimation or death. Little is known on how these opposed events are coordinated and we believe that the different temporal patterns in signaling provide new insights to dissect adaptive from damage related events.

The manuscript has not been published previously, is not under consideration elsewhere, and all of the authors have approved publication.

Please address all correspondence to:

Dr Alice Trivellini

Life Science Institute

Scuola Superiore Sant’Anna

Viale delle Piagge 23, 56124

Pisa, Italy

E-mail: alice.trivellini@gmail.com

We look forward to hearing from you.

Sincerely,

Alice Trivellini

Dear Editor,

Thank you for very useful suggestions on the manuscript. We agree with all your suggestions, and therefore, incorporated in the revised MS. Below you will find our responses to your suggestions. We addressed all the comments of editor in the notes below. Please note that the editor comments are shown in **bold type (E)** and our responses in plain type (A).

Regards, The Authors.

Editor comments

E 1) Please shorten Highlights as per journal's style (4 separate, short sentences should be given, see previous published articles in the same journal for reference)

A 1) As suggested by the editor the highlights were rewritten considering the journal style.

E 2) Please include separate subheadings to better separate ideas in the discussion section (see also previous published papers to follow journal style)

A 2) As suggested by the editor we included in the discussion section subheadings to better separate the different concepts. The journal style was considered.

E 3) Please include more citations in your discussion, e.g. on the ABA/Ethylene interplay in salinity response through ERFs, or on the role of ABA on proline biosynthesis, among others. Please make a final effort to highlight your most important discoveries in the Discussion section making reference to other studies in the field. Yours is really a very good piece of work, please highlight your work to make it attractive to potential readers.

A 3) We are really thanks for this suggestion. We rewrote the discussion and we tried to highlight the most important and novel ideas. We focused mainly on 4.1. The osmotic tolerance's players and on ABA/Ethylene interplay in salinity response through ERFs (4.3. subparagraph). We also partially rewrote the conclusion as well. Please let us know if we satisfied your suggestion, otherwise we can try to improve this section more.

E 4) Please do not mention twice the number of replicates in Fig 1 legend (is it 5 or at least 5?)

A 4) Thank you for the comments, we corrected the legend of figure 1.

The authors thanks the Editor and the Reviewers for the valuable and very helpful comments that undoubtedly have improved our manuscript so far.

With Best Regards

Alice Trivellini

Highlights

- The complex molecular and physiological mechanisms of NaCl tolerance in *Antirrhinum majus* L. were dissected using a two-mode model, survival versus death and a multi-step experiment.
- Tolerance to the osmotic phase was associated to a better integration and transduction of NaCl stress into growth programs.
- The transcriptional reprogramming of Ca^{2+} signaling components were pivotal to modulate differential abilities to tolerate the salt.
- ABA and ethylene signaling pathway act as a positive regulators of salt acclimation.

*Manuscript
Click here to view linked References

SURVIVE OR DIE? A MOLECULAR INSIGHT INTO SALT-DEPENDANT SIGNALING NETWORK

Alice Trivellini[1]*, Mariella Lucchesini[2], Antonio Ferrante[3], Giulia Carmassi[2], Guido Scatena, Paolo Vernieri[2], Anna Mensuali-Sodi[1]

[1] Institute of Life Sciences, Scuola Superiore Sant'Anna, Pz. Martiri della Libertà 33, Pisa 56127, Italy

[2] Department of Agriculture, Food and Environment, Via del Borghetto 80, 56124 Pisa, Italy

[3] Department of Agricultural and Environmental Sciences, Università degli Studi di Milano, I-20133, Italy

*corresponding author. alice.trivellini@gmail.com

Abstract

The response of plants to salt stress involves dynamic changes in growth and signaling leading to successful adaptation or death. To elucidate how these opposed events are coordinated we identified a salt-tolerant (*obesifruticosa*) and a salt-sensitive (*aestiva) Antirrhinum majus* mutants using shoots as sensitive indicator of stress magnitude. A series of physiological tests were performed that compared the response after 6 hours and 3 days of these contrasting mutants grown in agar under a single (200 mM) NaCl concentration, including shoot area, root length, relative water content, plant height, and overall biomass accumulation. Additional measurements of ABA content, chlorophyll degradation, ethylene production, net photosynthesis rates and Na^+, K^+, Ca^{2+}, and Mg^{2+} content were also reported. RNA-seq analysis was performed on the two mutants after 6 hours and 3 days under 200 mM NaCl. A total of 9199 transcripts were found to be differentially expressed in response to NaCl treatment in the two mutants. A large collection of known genes, including MAPKs, CDKs, CDPKs, CIPKs, various transcription factors, various ion transport proteins, and various genes involved in ABA and ethylene signaling pathways were described in detail that displayed differential expression profiles. Overall these data provided evidences of a putative osmotic tolerance sensing and signaling mechanism through a better integration and transduction of environmental cues into growth programs. The reprogramming of calcium-signaling components generates specific stress signatures affecting differentially the salinity tolerance traits such as tissue tolerance and anion exclusion. Interestingly, the hormones ABA and ethylene may action as a positive regulators of salt acclimation by the modulation of their signal transduction pathway.

1. Introduction

High salinity is considered to be the major environmental factor limiting plant growth and productivity (Munns and Tester, 2008).

High NaCl levels expose the plants to two distinct stress components: an osmotic and an ionic (Munns and Tester, 2008). As a result of osmotic stress, water potential is reduced and a complex response involved in limiting cellular damages and reaching a new homeostasis, is triggered in plants, through the coordination of several physiological changes such as stomata closure, alterations of cell growth and photosynthesis inhibition (Zhu, 2002). The ionic component of salt-

stress is attributed to the toxic effects of Na^+ and Cl^-, increasing the levels of Na^+ and Cl^- in the cytosol which imbalances the intracellular K^+/Na^+ ratio and the homeostasis of other ions like Ca^{2+} (Blumwald et al. 2000). The mechanisms involved in sensing and transmitting both osmotic and Na^+ are extremely important to cope with salinity stress and those sensory modalities are crucial for adaptation (Denlein et al., 2014; Roy et al., 2014). Three main mechanisms of salinity tolerance exist in plants: osmotic tolerance involved in limiting shoot growth with and not well understood sensing and signaling mechanisms; then ion exclusion by reducing the accumulation of toxic ions using translocation and remobilization systems to reduce their accumulation in the cytosol; and tissue tolerance which involves the sequestration of toxic ions into the vacuoles (Roy et al., 2014; Julkowska et al., 2016). Plant hormones are known to play key roles in regulating ionic homeostasis and plant salt tolerance (Wu et al., 2008; Ferrante et al., 2011). For example, salt-induced abscisic acid (ABA) levels activates ABA-dependent signaling pathways (Zhu, 2002), which in turn controls the salt-stress responses at transcriptome level, leading to adaptation (Xiong et al., 2001). Also ethylene and its signaling pathways play crucial role in plant salinity stress adaptation, as shown by the increased salt tolerance of transgenic plants overexpressing ethylene response factors (ERFs) and others mutants deficient for ethylene sensitivity having on the contrary higher salt-sensitivity (Zhang et al., 2012; Achard et al., 2006).

Here, we used forward genetics with modern genomics to discover molecular and physiological traits that contribute significantly to salinity acclimation in *Antirrhinum majus* L.. *A. majus* is a glycophyte perennial native to the Mediterranean region with a large range of mutants available at IPK gatersleben germplasm bank (https://gbis.ipk-gatersleben.de/). This species was used as a model system to study the morphology and the symmetry of flowers (Schwarz-Sommer et al., 2003) and in our work it was studied to identify novel acclimations to salinity stress.

A genetic screen *in-vitro* using shoots as sensitive indicator of stress tolerance for salt-stress was carried out (Claeys et al., 2014; Dinneny 2015), to selected two mutants by comparing their behaviour (sensitive versus tolerant). Then we investigated the physiological alterations as well transcriptional regulation by next-generation-RNA-sequencing technologies (RNA-seq) evaluating temporal dynamic changes (six hours versus three days). Our observations provide understanding of how the salt stress promotes the survival or the death by investigating molecular activities underlying these outcomes.

2. Materials and methods

2.1. Plant material

Seeds of *Antirrhinum majus* (L.) were obtained from GBIS/I (http://www.ipk-gatersleben.de/en/genebank/, Genebank Information System of the IPK Gatersleben, Germany). The mutant's details are reported in Supplementary Table S1 and S2 and further information can be obtained from the above website as well as from snapdragon database (http://www.antirrhinum.net/).

2.2. Screening of A. majus mutants

In the first step experiment (Fig. S1), 62 mutants were screened for NaCl-sensitivity using a root bending assay previously described for Arabidopsis by Wu et al. (1996). The seedlings were grown

under an 8:16 h, dark:light (100 µmol-1$m^{-2}s^{-1}$) at 22°C. Five day after germination, the seedlings with 1- to 4 cm-long roots were transferred in squared plates onto MS/2 half-strengh supplemented with increasing concentration of NaCl: 0, 50, 100, 200, 400 mM for the preliminary test with wild type and 0, 100, 300 mM for the mutant screening. The plates, with seedling arranged in row, were oriented vertically with the roots pointing upward. Roots that did not show curving and apparent growth were noted, as well as the seedling color (bleaching of cotyledons or not; Table S1). Then, the mutant seedlings from control plates were picked up and the shoots micro-propagated and used for the second step experiment (Fig. S1).

2.3. In vitro growth conditions

Germinated plantlets without roots were sub-cultured on MS medium containing 0.25 mg/L BA and the developed shoots were used for salt-stress experiments. For NaCl treatments, similar size apical shoots of the selected mutants were transferred in vented Magenta® vessels (nine explants/mutant) with MS medium without both PGRs and sucrose, supplemented with NaCl at the following concentrations: 0, 100 and 200mM. The apical shoots (explants) were sampled and collected for downstream morpho-physiological and molecular analysis, respectively after 21 d (Fig. S1, second step experiment) and 6h-3d (Fig. S1, third step experiment). At least four replicate vessels were used for each treatment.

2.4. Growth and water content

The height and water content parameters were determined after 21 days. Water content was calculated as the difference between fresh weight and dry weight of each sample. Dry weight was determined after drying the samples in ventilated oven at 72°C for 4 days.

Height reduction and water loss were calculated using the following equation:

% = 100 (1 – S/C) where S and C are the values of each parameter, respectively, in the salt-stressed shoot and in the controls.

2.5. Mineral content and seedling pigments

Dried samples were mineralized (60 min at 220 ◦C) using nitric and perchloric acids. Sodium (Na), potassium (K), calcium (Ca), and magnesium (Mg) were determined using an atomic absorption spectrometer (Varian AA 24FS, Australia): three samples, each consisting of 10 individual shoots, were analysed for each treatment.

Total chlorophyll and anthocyanins were determined spectrophotometrically following Lichtenthaler (1987) and Kho et al. (1977) methods, respectively.

Pigment degradation percentage was calculated using equation 1 based on the measurements on the salt-stressed (S) and the control (C) plants.

2.6. free ABA and measurements of ethylene and CO2

Explant samples were collected, weighed, frozen in liquid nitrogen and then stored at –80 °C until analysis. ABA was determined by an indirect ELISA based on the use of DBPA1 monoclonal

antibody, raised against S(+)-ABA (Vernieri et al., 1989). The ELISA was performed following Trivellini et al. (2011b).

Ethylene and CO_2 concentrations were measured using an HP 6890 gas-chromatograph (Hewlett Packard, Milano, Italy) as reported in Kiferle et al (2014). The instantaneous rate of net photosynthesis (PN; µM s^{-1} g^{-1} DW) and the ethylene release (pM s^{-1} g^{-1} FW) was calculated as reported by Fujiwara et al. (1987) and Kiferle et al. (2014). Air samples (2 cm^3) were taken from the head-space of culture vessels (at least five replicates, each consisting of an individual vessel).

2.7. RNA-Seq analysis and functional annotation

Tissue sample and RNA isolation – To reduce plant to plant variability, each sample was created by pooled together 12 different shoots from six different magenta growing-box, deriving from at least three independent experiments. To avoid the effects of circadian rhythm on gene expression patterns, the harvesting shoots occurred at the same time of day (after 6 h in the photoperiod). The samples from control 6h and control 3d of each mutant were pooled together. Samples were immediately frozen in liquid nitrogen and stored at -80°C. Total RNA was extracted with Spectrum™ Plant Total RNA Kit (Sigma-Aldrich, Italy) according to the manufacturer's instructions. The extracted RNA was treated with RNasefree DNase I (Takara) following the manufacture protocol.

RNA purity and integrity were assessed by Agilent 2100 bioanalyzer-RNA 6000 NanoChip (Agilent Technologies) and concentration by Nanodrop 8000 (Thermo Scientific). 5 µg of RNA with A260/A280 ≥ 1.8 and RNA integrity number (RIN) ≥ 7 were used for RNA-Seq. Paired-end library preparation, Illumina sequencing and de-novo assembly were performed by staff at the Institute of Applied Genomics (IGA) (Udine, Italy; details are reported in Supporting Information Table S13).

BLAST alignment, GO terms mapping, rpsblast to enzymes and pfam domains were obtained with FastAnnotator (Cheng et al., 2012; http://fastannotator.cgu.edu.tw/analysis.php#page=upload).

In each library, the expression level of each contig was estimated by counting the number of all the clean reads that mapped to that transcript. The raw gene expression counts were then normalized using the RPKM method and a threshold of RPKM ≥ 3 was set to define transcriptionally active genes within a library (O'Rourke et al., 2013). Statistical analysis for differential expression between the control and treated samples was performed according to Beneventi et al. (2013) with the R package EdgeR (http://www.bioconductor.org/packages/2.12/bioc/html/edgeR.html) by setting a threshold of 10 mapped reads per transcript. A nominal average dispersion value was set to 0.25 (Biological coefficient of variation; BCV = 50%; McCarthy et al., 2012) and the counts distribution of each gene was expressed as the logarithm of the fold-change (FC) ratio between control and each treated sample. We used FDR ≤ 0.05 and the absolute value of Log2 fold change (FC) ≥ 2 as the threshold to determine the significant difference in gene expression. Heatmap was generated in R with 'hclust' function using Euclidean distance (R2.14.1, http://www.R-project.org). The multidimensional scaling plots (MDS), were performed through the "plotMDS.dge" function of edgeR package. In addition, manual filtering of expression patterns was performed to identify genes that fit user-defined terms reported in Tables S3-S12. These gene lists were used to create additional heatmaps implemented with R-package: 'hclust', complete method and euclidean distance.

2.8. qRT-PCR validation

Total RNA was isolated using TRIzol reagent (Invitrogen) as described by Yoo et al. (2004). RNA (1 µg) was treated with DNase1 (Takara) and used as a template for cDNA synthesis using SuperScript III (Invitrogen) and the reverse-strand primer KS-DT (listed in Supplemental Table S10). The cDNA was diluted 20-fold and qRT-PCR was performed in 10-µL reactions using a LightCycler 480SYBR-Green1 Master PCR-labeling kit (Roche) and Rotor-Gene6000 RealTime-PCR machine (Corbett Research). Primers were designed using QuantPrime (Arvidsson et al., 2008), www.quantprime.de/) and are listed in Table S4. PCR was performed on three biological replicates with five pooled shoots each. Analysis was carried out using the method of 'comparative quantification' present in the Corbett Rotor-Gene6000 Application Software (McCurdy et al., 2008; Trivellini et al., 2012). The amplifications were normalized to cyclophilin (contig_7590), and actin (contig_17403), reference genes which are particularly stable throughout a wide range of environmental stresses (Nicot et al., 2005).

2.9. Statistical analysis

The data were subjected to statistical analysis using PRISM 6 software (GraphPad Software, San Diego, CA, USA). To stabilize variance and normalize percentage data, the arcsine transformation was used. Two-way ANOVA were carried out to analyze the effects of salt concentrations among *A. majus* mutants, and comparison among means values were separated using the Bonferroni multiple comparison test ($P \leq 0.05$). Student's t-test was used to compute the pair-wise comparisons between group means. Each experiment was repeated at least twice.

3. Results

3.1. Isolation of mutants with differential sensitivity to salt stress

A three-step experiment was set up in order to screen 62 mutants of *A. majus* to discover critical molecular and physiological traits that contribute significantly to salinity acclimation. The pipeline of the different steps are summarize in Fig. S1.

A. majus is sensitive to low/moderate levels of NaCl stress. The sensitivity to NaCl was determined by conducting dose-response experiments using snapdragon wild-type growing at different NaCl concentrations over two weeks. As, upon NaCl excess, root growth, shoots growth and visual bleaching/de-greening of leaves are easily visual assessed *in vitro* using a root bending assay modified from Wu et al. (1996) (Fig. S2).

Since 200mM is considered a key concentration point for the classification of halophytes in: plant tolerant with growth reduction (these plants grow slowly up to maximum 200 mM) or tolerant (these plants grow fast and can tolerant concentration up to 500mM), (Flowers et al., 2015), we performed a genetic screen for mutants exhibiting morphological and physiological features linked to salt stress-responsive phenotypes using two NaCl concentrations, one above (300 mM) and one below (100 mM) the threshold of 200mM. 62 mutant's lines were transferred onto vertical plates and the different phenotypes under salt stress were visually assessed (Table S1). Among them we selected 12 genotypes, which were further characterized for their response to salinity stress after long-term exposure (21 days) (Table S2). Among them, we identified two snapdragon mutants which had marked differences in sensitivity to high NaCl: *obesifruticosa* (*of*) was more tolerant and

aestiva (*aes*) was more sensitive. More details on screening procedure are reported in Fig. S1, Fig. S2 and Tables S1, S2. One week after being transferred in 100mM NaCl, although there was no detectable differences between the root growth of *of* and *aes*, the shoot area was markedly reduced in *aes* and seedlings were completely bleached (Fig. 1a). On the contrary, *of* seedlings showed green cotyledons even also on 300mM NaCl (Fig. 1b).

Then, the apical shoots were exposed to the dose limiting shoot growth (200mM NaCl) for 21 days assuming that the shoots had recovered from osmotic shock and the ionic phase of salt stress had started (Munns, 2010). After 21 days, there were extreme phenotypic differences between *of* and *aes*. Shoot height of both mutants at 200mM NaCl was progressively reduced and this was less evident in *aes*, which showed reduction of 40% against 60% in *of* (Fig. 1a). Relative water loss and shoot growth reduction (DW) was more pronounced in *aes* (-75% and -73%) compared to that showed by *of* (-46% and 24%), (Fig. 1a). *of* had less pigments reduction with percentages of chlorophyll and anthocyanins degradation of 40 % and 25 %, respectively; whereas pigments were almost completely degraded (98 %) in *aes*. (Fig. 1c).

3.2. Salinity triggers two qualitatively different physiological responses

To gain further insight into the salt response network between these opposed mutants, *aes* and *of* shoots were evaluated after 6 hours and 3 days of salt-stress, considering that the flexibility to environmental changes depend on time which the organism handle to adapt or died. The decrease in chlorophyll content was stronger in *aes,* reaching maximal chlorophyll degradation percentage around 60 % and a more severe bleached phenotype after 3 days, than *of* (Fig. 2a, b).

In *of* and *aes*, ABA accumulation peaked at 6h of salt treatment. In *aes* the ABA levels was double to those reported for *of*, but after 3d it sharply decreased (Fig. 2c). These data indicated that ABA biosynthesis was dynamically regulated with peak levels associated with the early phases of the salt stress response in both mutants. Salt-induced ethylene production was evident for both mutants after 6h. Ethylene level returned similar to control in *aes* after 3d, instead at the same time-point increased in *of* (Fig. 2d). Interestingly, the levels of ABA and ethylene in tolerant mutant was higher during the entire experiment suggesting that these hormones positively regulate salt tolerance (Peleg and Blumwald, 2011).

In our systems, the photosynthetic rate after 6h of salt-stress was strongly reduced only in *of* (Fig. 2e). The assimilation of CO_2 after 3d was invariably lower in *of* than in *aes*, suggesting the ability to maintain a low energy–consuming status, by fixing less CO_2 (Jacoby et al., 2011) (Fig. 2f). We reported evidences that respiratory homeostasis in the shoot is linked to salt tolerance, suggesting that the prevention of damage to the photosynthetic machinery by CO_2 fixation appear to have the priority over the mechanism of growth as previously had been shown for *Triticum* (Kasai et al., 1998).

Na^+ and K^+ homeostasis is critical for salt tolerance but also Ca^{2+} and Mg^{2+} are important nutrients in plants exposed to salt-stress. The concentration of measured ions, showed accumulation of Na^+ after 6h in shoots of both mutants (Fig. 3a). Shoots of *of* accumulated more Na^+ after 3d as compared with *aes*. The K^+ concentration in *aes* increased after 6h, but after 3 days of salt stress its retention ability decreased. In contrast, accumulation of K^+ in *of* shown an increasing trend between the time-points (Fig. 3b). The increase in Ca^{2+} and Mg^{2+} was significantly evident in *of*

after both 6h and 3d of salt stress, whereas the values in *aes* did not show any differences (Fig. 3c-d). Therefore, greater salt sensitivity of *aes* was associated with its incapacity of maintaining a proper cellular K^+/Na^+ homeostasis.

3.3. De novo mRNA-seq assembly and annotation of transcripts

Significant morpho-physiological differences were shown at different sampling time in response to salt between these genotypes, which lead us to investigate how temporal shifts of salt-stress signals can generate different transcriptional signatures. We therefore selected the 6h and 3d time-points to deeply elucidate the molecular mechanism underlying survive versus die mode. RNA-Seq libraries were generated and pair-end sequenced using the Illumina Hiseq™2000 platform from *of* and *aes* shoots under 200mM NaCl and their controls. The results of de-novo transcriptome assembly are summarized in Fig. 4a. High-quality reads deriving from all libraries were used to de-novo assemble the *A. majus* transcriptome generating 49298 contigs/transcripts, with a mean length of 844.01 bp. The size distribution of contig length is shown in Fig. 4a. The high N50 value (1391 bp) and the GC content (39.02 %) similar to that of other plant species like *Arabidopsis thaliana* and *Cassia angustifolia* (Victoria et al., 2011; Reddy et al., 2015) indicated a good quality assembly. The blast similarities included more than 30 plant species and the BLAST top hit species distribution is shown in Fig. 4b and the results obtained from annotation are further described in Fig. S3, S4 and S5.

3.4. Transcripts differentially regulated in *aes* and *of*

A total of 9199 transcripts were differentially expressed in response to NaCl stress in the two mutants (Table S3, Fig. 5a). Much less genes have changed their expression in response to NaCl in *of* than in *aes* and the number of down-regulated genes was higher in *aes* than in *of* (Fig. 5a). Multi-dimensional scaling (MDS) plot of the count data clearly separated the libraries into five groups (Fig. 5b), three independent groups for *aes* and two for *of* (ctrl+3d-NaCl and 6h-NaCl) suggesting adaptation for *of* and a cell death mode for *aes* mutant which take the distance from its ctrl. Heatmap illustrating expression patterns of various subgroups of differentially expressed genes (DEGs) were generated in R with 'hclust' function (Fig. 5c) and the DEGs of each cluster were analyzed using KEGG Orthology Based Annotation Systems (KOBAS), (Fig. 5c; Table S4), (Wu et al., 2006; http://kobas.cbi.pku.edu.cn/program.inputForm.do?program=Annotate) to identify significantly enriched pathways (FDR correction: Corrected P-value ≤ 0.05). Three of these clusters contain KEGG pathways significantly upregulated, whereas four of these clusters contains the significantly downregulated ones (Fig. 5c). Many typical stress-affected symptoms such as photosynthesis-antenna proteins, photosynthesis, and carbon fixation and components of cell cycle machinery and DNA replication were significantly overrepresented in the downregulated pathways. Certain signaling modules that links and transduce environmental and developmental cues into intracellular responses were significantly enriched in the upregulated genes, such as MAPK and cAMP signaling pathway. Meanwhile, plant hormone signal transduction pathway was obvious activated in the upregulated genes. These results suggested that these pathways might pertain to cell survival or cell death.

The expression levels of 13 genes were assessed using qRT-PCR to validate the RNA-seq results (Fig. S6; Table S5). Among these 13 genes, 2 genes were housekeeping genes and 11 genes were up, down-regulated or did not change in the two genotypes in response to salt stress at 6 hours

and 3 days. Correlation between RNA-seq and qPCR gene expression profiles was reported in Fig. S6, indicating that our RNA-seq results were reliable.

3.5. Sensory mechanisms

Of the 9,199 transcripts differentially expressed in response to NaCl, 447 were identified as kinases (Table S6), which play important roles in regulating the stress signal transduction pathways (Lehti-Shiu and Shiu, 2012). The RLK/Pelle family is the largest families responding to NaCl stress identified in both mutants (Fig. 6a; Fig. S7). This family has an important role in plant growth, development, stress responses and are linked to the early steps of osmotic-stress signaling in a variety of plant species (Osakabe et al., 2013).

We found three kinases families whose expressions were specific to *of* tolerant mutant: the AMP-activated protein kinase (AMPK)/SNF1 (sucrose-non-fermenting1), NIMA-related kinases (NEK1 and NEK6, contig_43308 and contig_800) and a MAPK2K exclusively down-regulated in *of* (contig_32338).

The cyclin-dependent kinases (CDKs) transcripts as well as three transcripts belonging to the plant specific TKL family exhibit distinct expression patterns between the two mutants. After 6h of salt-stress in *of* two HIGH TEMPERATURE1 isoforms (TKLs), which normally regulates stomatal response to CO_2 (Hashimoto et al., 2006) were up-regulated whereas in *aes* after 3d were down-regulated. A homologue of CDKE1 was highly induced (7-fold, contig_26954) in *of* after 6h of salt stress. CDKs are core cell cycle regulators and, changing environmental conditions, negatively affected the growth and cell cycle (Kitsios and Doonan, 2011). Important mitotic checkpoints were differentially regulated in *of* by candidates like KIP PROTEINs (contig_37036 and contig_38206, Table S6) which inhibit CDKs (Rymen and Sugimoto 2012). Moreover, the transcriptional induction of RAPTOR (over 6-fold; contig_24585) and the two SNF1 related kinases (over 2 and 6-fold) in *of* may be required for growth inhibition as well as to maintain energy homeostasis by the activation of the energy-sensing kinases (Nietzsche et al., 2016).

The cytosolic calcium increase is one of the earliest responses of plant cells to stress treatments, and calcium-binding proteins with their activated kinases are required for several stress responses (Reddy et al., 2011). Up-regulation of genes encoding Ca^{2+} sensors, including calcium-dependent protein kinases (CDPKs) and calcineurin B-like (CBL)–interacting protein kinases (CIPKs) has been reported uniquely in the tolerant mutant (Fig. 6a, Table S6, Fig. S8). Several families of proteins, including the glutamate receptor family (GLRs), the cyclic nucleotide regulated channels (CNGCs), annexins (ANNs) and mechanosensitive channels (MSC) are affected transcriptionally by salt stress in both mutants (Fig. 6b, Fig. S9) and the majority of them were upregulated in the tolerant mutant after 6h. Through the stress activation/repression of Ca^{2+} channels, respectively in *of* and *aes* shoots, the organism can modulate different calcium-dependent downstream responses. In detail, two CBL interacting proteins, three CIPKs and NHX were down-regulated in aes suggesting worst performance to detoxify Na^{+}. In contrast, *of* transcripts were mostly up-regulated. Interestingly, a CDPK17 was differentially regulated between the mutants, strongly induced in *of* and severe repressed in *aes* after 3 days. Overall, these findings might suggest an alternate or defective Ca^{2+} signaling pathway which modulate the differential sensitive to NaCl between hours and days of exposure.

3.6. Transcriptional control

Transcription factors (TFs) are essential by coupling sensory mechanisms of salt stress to the acclimation responses. We grouped a total of 338 DETs under salt-stress (Table S7) in the two mutants into 39 TF families (Fig. 6c). The ETHYLENE RESPONSE FACTOR (AP2_EREB) and NAC families are the largest family responding to NaCl stress identified in both mutants, followed by basic helix-loop-helix (bHLH). Other core sets of TF families include basic leucine zipper (bZIP), WRKY, MYB, and Homeobox. The transcriptional regulation was mostly repressed in the *aes* showing the highest number of TFs down-regulated after 3d, especially for the bHLH, MYB and Homeobox families. Other families were induced late like WRKY, NAC and AP2-EREB. All the major TF families regulated by salt are directly related to either a general stress response such as bHLH, NAC, MYB, and WRKY or a specific hormone pathway (AP2-EREBP) (Aprile et al., 2009; Walia et al., 2009; Dugas et al., 2011, Peng et al., 2014; Guo et al., 2015).

Moreover, salt-stress in *aes* caused a reduction in the transcript levels of the Growth-Regulating Factors (GRFs) such as GRF1, GRF2, GRF3, GRF8 even over 8-fold after 3d (GRF1; contig_34930). However, little is known about the signaling networks that relate salt responses to cell cycle progression. Here, the strong transcriptional repression of two atypical E2F TFs, E2FE and DP-E2F-LIKE1 (over 4 and 7-fold; contig_35795 and contig_10612) in *of* probably contributed to its greater salt tolerance. Finally, four members of nuclear factor Y (NF-Y) TFs family, were only down-regulated in *aes*. This family is involved in many developmental stress-responsive processes in plant (Petroni et al., 2012; Ha et al., 2013; Ma et al., 2015; Palmeros-Suárez et al., 2015).

3.7. Network of Na and K transport

A total of 342 transcripts known to be involved to re-establish and maintain ion and cellular homeostasis were differentially expressed in the two genotypes in response to salt-stress (Table S8). We identified transcripts related to network of potassium transport systems and its regulation (Fig. 6b, Fig. S10, Fig. S11) (Shabalaa and Pottosin, 2014). Five transcripts for outward-rectifying K^+ channels (KORs and GORK) mediating potassium efflux from the cell were differentially regulated by salt, two of them (contig_15839 and contig_16713) were high up-regulated (over 7 fold) after 6h in *of*, and the others were down-regulated more than 2-fold in *aes*, (contig_32478; contig_2021). Additionally, a two-pore K^+ channel (TPK/KCO) was up-regulated in *of* after 6h and repressed in *aes* after 3d; and a further two TPKs transcripts were again repressed in *aes*.

Several genes encoding for Ca^{2+}-ATPase enzymes, were strongly and only upregulated in *aes* (Fig. S10), suggesting a defective calcium waves leading to higher sensitivity to NaCl stress.

High-affinity potassium transporters (HKTs and KTs) were up-regulated over 6-fold after 6h in *of* and mainly repressed at different time-points in *aes* (Fig. 6c). Another important group of ion transporters are the monovalent cation/proton antiporters (CPAs) (Chanroj et al., 2012), whose members include the cation/H+ exchangers (CHXs), the K^+ efflux antiporter (KEAs) and the Na+/H+ antiporters (NHXs). In our study, a KEA transcripts was strongly upregulated in *of* after 6 hours (contig_30952) and the others two were dowregulated in *aes* after 3 days (contig_11463 and contig_14323). A NHX transcript was strongly down-regulated over 7-folds (contig_29086) in *aes*.

Moreover, a gene encoding membrane protein that mediates guard cell anion efflux, an homologues of the SLOW ANION CHANNEL-ASSOCIATED1 (SLAH1, contig_22831) was 4-fold up-

regulated after 6h only in *of*. Interesting, a member of the aluminum-activated malate transporter (ALMT2, contig_34048) was strongly down-regulated in *aes* at both timing.

3.8. ABA and ethylene signaling pathway in salt-stress

We identified DETs related to the central stress-player hormones, ABA and ethylene (Table S9 and S10, respectively). Many transcripts associated with ABA signaling showed significantly differential expression under NaCl stress (Table S9). The expression of two PYR/PYL/RCAR homologs were repressed in the sensitive mutant, while most transcripts encoding protein phosphatases-2Cs (PP-2C) were induced in both mutant at different salt-treatment time points. Two SNF1-related protein kinase regulatory subunit beta3 and gamma1 transcripts were up-regulated by salt in *of* at 6h (contig_18876 and contig_22886), and only a single homolog of SnRK2 was down-regulated early in response to NaCl in *of*. Eight 9-cis-epoxycarotenoid dioxygenases (NCEDs) transcripts were mainly up-regulated in both mutants after 6h, with shared differential expression for NCED3, being also one of the most up-regulated genes in the pathway (contig_27065; Table S10). Thus, consistent with the rate-limiting activity of NCEDs in ABA biosynthesis and the observed timing of ABA levels peak (Fig. 2d), NCED3 is likely having an essential role in salt stress-induced ABA accumulation in agreement with previous studies (Barrero et al., 2006; Geng et al., 2013). The transcriptional regulation of ABA degradation with its conversion to phaseic acid by three ABA 8'-hydroxylases transcripts showed a similar temporal trend as NCED3. This may indicate that synthesis and degradation pathways are tightly co-regulated, as also suggested by Geng et al. (2013). ABA biosynthesis sharply decreased in *aes* but it didn't change significantly in *of* after 3 days of salt stress, probably due to the decrease in the transcript levels of genes involved in carotenoid biosynthesis, which were largely down-regulated in the sensitive mutant (Table S9).

Many genes involved in ethylene biosynthesis and signal transduction (Table S10; Fig. S12) were induced or repressed in response to salt stress in both mutants. Six 1-aminocyclopropane-1-carboxylic acid (ACC) synthase genes (ACS) and ten ACC oxidase (ACO) involved in ethylene biosynthesis were identified and in *of* were all up-regulated after 6h, consistent with observed rise in ethylene level (Fig.2d, Fig. S12). However, none of these transcripts was significantly induced at 3d, despite the ethylene production increased (Fig. 2d, Fig. S10). Thus, plants experienced stress after 6h and this condition was enough to induce high ethylene accumulation during the first days of salt exposure. Instead, in *aes*, despite the reduced ethylene production manifested after 3d of salt stress, its biosynthetic transcriptional network at this time-point still remain induced with five ACS transcripts upregulated.

4. Discussion

Based on our analysis, we propose a signaling network underlying NaCl-dependent responses in snapdragon mutants (Fig. 7). Here we have attempted to focus on the mechanisms of traits that are hypothesized to contribute to salinity tolerance. Results showed that a better salinity tolerance of snapdragon, can be achieved as following.

4.1. Osmotic tolerance's players

The plant growth adaptation to stress, particularly to salt, is actively and precisely reprogram by cell cycle progression, and needs the regulation of mitotic checkpoints (Juraniec et al., 2016).

Recently, the TARGET-OF-RAPAMYCIN1 (TOR1) protein has been found to coordinate and control developmental transition and growth through the stimulation of cell cycle entry (Xiong et al., 2013). TOR1 is a highly conserved kinase that integrates nutrient and energy signaling to promote cell proliferation and growth (Xiong et al., 2013). In snapdragon tolerant mutant, the TOR-(Target of Rapamycin)-binding partner regulatory-associated protein of TOR (RAPTOR), which was required for suppression of TOR activity leading to cell-cycle arrest induced by energy stress (Gwinn et al., 2008), was upregulated. These data suggest, that *of* efficiently switch between the normal growth metabolism involved in cell proliferation and growth, where TOR is the master regulator by the transcriptional activation of its repressor RAPTOR and concomitantly the induction of SNF1 kinases which on the other hand are essential in response to stress to preserve vital resources through the inhibition of growth and development. Baena-González et al. (2007) demonstrated the pivotal roles of KIN10/11, a SNF1-related protein kinases, in linking stress, sugar and developmental signals to function dynamically in the network controlling growth and survival. Moreover, the upregulation of a NIMA-related kinase (NEK6) was also an important node that links the stress signal with plant metabolism and promotes stress tolerance (Zhang et al., 2011). These authors demonstrated that NEK6 transcript and protein were induced by the ethylene precursor ACC and salt stress, and promoted plant tolerance to osmotic and salt stresses. The reprogramming of cellular growth under adverse conditions strongly influences the fate of plants and represents a critical switch: survival versus death mode. Salt-stress in *aes* caused a reduction in the transcript levels of the GRFs. Interestingly, the independent overexpression of GRF1 and GRF2 was reported to increase the cell size (Kim et al., 2003) thus suggesting that in *aes* could be present a mechanism for the de-activation of cell expansion (Omidbakhshfard et al., 2015). In contrast, in *of* plants, the transcripts encoding for the xyloglucan-endotransglucosylases/hydrolases (XETs; Table S11) were highly up-regulated and this suggest that these components are central in modifying the cellular expansion under stress (Cosgrove, 2005). However, little is known about the signaling networks that regulate salt responses to cell cycle progression. A closer look on transcriptional reprogramming, suggested that in *of* was retarded the progression of cell cycle, by candidates like KIP PROTEINs (contig_37036 and contig_38206, S6) which inhibit CDKs (Rymen and Sugimoto 2012). These inhibitors suppresses the transition through the different cell cycle phases mediated by the CDKs. Recently was demonstrated that one of the major physiological activity of cell-cycle inhibitors such as Cip/Kip families is to prevent replicative stress during development by reducing the susceptibility to tumor development (Quereda et al., 2016). Another class of cyclin-dependent kinase inhibitors SIAMESE-RELATED 5 (SMR5) and SMR7 have been shown to pause the cell cycle in response to ROS-induced DNA damage (Yi et al., 2014). Thus, CDK inhibitors such as KIPs and SMRs seems to help in shaping and adapting plants under different stressful environments.

Interestingly, potentially the reduced cell numbers caused by checkpoints activation might be compensate by an increase in DNA ploidy level driving cell enlargement, as reviewed by Cools and Veylder (2009). In fact, osmotic stress alters the metabolism of gibberellin with a consequence of DELLA destabilization, which prompts the early onset of endocycle where mitosis is skipped and consequently cell division is omitted by the transcriptional reduction of DP-E2F-LIKE1 (DEL1) (Claeys et al., 2012). The transcriptional repression of two atypical E2F TFs, E2FE and DP-E2F-LIKE1 might improve DNA repair abilities in the tolerant genotypes as reported for Arabidopsis plants knocked out for E2Fe/DEL1. These plants under unfavorable environmental conditions, showed an enhanced ability to compensate the stress-induced reduction in cell number by ploidy-dependent cell growth (Radziejwoski et al., 2011). Moreover, the analysis of DETs induced by salt stress in snapdragon mutans, identified four NF-Y TFs which generally are involved in the stress-response

during development (Petroni et al., 2012; Ha et al., 2013; Ma et al., 2015; Palmeros-Suárez et al., 2015) suggesting again the existence of a genetic plasticity in the control of growth response under unfavorable conditions (Claey and Inzè, 2013).

Here, we provide evidences about an osmotic tolerance signaling mechanisms performing a dual role under salt stress as it activates shoot growth reduction which results in an increased tolerance to NaCl. This osmotic phase, is much more closely associated with a better integration and transduction of environmental cues into growth programs (Fig. 7, i.e. regulators of growth and energy status). Plant checkpoints are nevertheless essential, because an improper response to stress can lead to hypersensitivity, and also because plants are sessile and through these regulators can balance between continuous growth and its arrest (Polyn et al., 2015). An example is the endocycle onset, which support the growth under adverse conditions by the duplication of the DNA content in the cell without division (Schoenfelder and Fox, 2014; Sholes and Paige, 2015).

4.2. Modulation of Ca^{2+} signaling by affecting salinity tolerance traits

A common feature of stress signaling pathways are the modulation of free calcium concentration, which generates stress specific calcium signatures (Schmöckel et al., 2015). These Ca^{2+} waves lead the regulation of various cellular responses involved in salt signaling pathway by several Ca^{2+} sensors such as calmodulin, CDPKs and CIPKs (Swarbreck et al., 2013; Pandey et al., 2015).

Calcium fluxes involved the activation of several protein families of Ca^{2+} channels, such as GLRs, CNGC, MSC and ANNs (Fig. 7, i.e. Ca^{2+} channels). These proteins have been shown to form Ca^{2+}-permeable channels allowing flow of calcium ions into the cytosol, which serves as a cue for environmental responses (Hou et al., 2014; Gilroy et al., 2014; Swarbreck et al., 2013; Laohavisit et al., 2013). Interestingly, in the tolerant mutant the MSCs, ANNs and CNGC were early transcriptionally induced by salt, whereas in *aes* were downregulated after both 6 h and 3 d. Thus, the stress-regulated calcium channels may be link the salt stimuli to calcium-dependent downstream responses through the regulation of several Ca^{2+} sensors, such as CDPKs and CIPKs (Julkowska and Testerink, 2015) (Fig. 7, i.e. Ca^{2+} sensors). The CIPKs contains a specific Ser/Thr protein kinase domain that is activated through interaction with CBL containing Ca^{2+} binding to phosphorylate downstream components and transduce Ca^{2+} signals (Luan 2009). The SOS pathway in Arabidopsis, containing SOS3 (a CBL protein as Ca^{2+} sensors), SOS2 (a CIPK) (Sanchez-Barrena et al., 2005), and SOS1 which is a Na^{+}/H^{+} antiporter (NHX) activated by SOS2 (Qui et al., 2004). The sensitivity of *aes* may be associated with its incapacity to detoxify the Na, suggested by the downregulation of genes associated with this defense system. On the other hand *of* mutant manifested a prompt activation of Ca^{2+} channels that may affect positively salinity tolerance. It's interestingly to note that the mutants did not share any overlap among the DEGs, except for CIPK17 that was differentially regulated between the two, strongly induced in *of* and severe repressed in *aes* after 3 days. Recently, the induction of CDPK17 in *Solanum commersonii* was linked to the mechanism of stress acclimation (Aversano et al., 2015).

Additionally, many genes encoding for Ca^{2+}-ATPase enzymes were strongly and only upregulated in *aes*. Cation transporters catalyse transmembrane movement of cations and are sustained by the proton force (Qi et al., 2014). The most potent factor in determining Ca^{2+} signatures, is the activity of Ca^{2+} efflux systems, such as Ca^{2+}-ATPases, that may be primarily involved in termination of Ca^{2+} signaling (Bose et al., 2011). Overall these findings suggest an alternate Ca^{2+} signaling pathway

493 with a possible surge of Ca^{2+} into the cytosol that targeted the downstream process involved in
494 tissue tolerance and anion exclusion.

495 Maintaining the optimal cytosolic K^+/Na^+ ratio is complex because it does not only depend from
496 Na^+ uptake or exclusion but is controlled by the K^+-release channels, such as KORs (Shabala and
497 Pottosin, 2014). A readjustment of Na^+ and K^+ among cell compartments of salt-grown barley
498 leaves seems to be an important strategy for maintaining K^+ activity constant and a high K^+/Na^+
499 ratio in the cytosol (Cuin et al., 2003). NaCl induced K^+ efflux occurs mainly via GORK, and a
500 reduction in its activity enhanced the tolerance to salt (Cuin et al. 2008) as we noticed clearly in *of*
501 by the down-regulation of GORK transcript (contig_34623) and a strongly up-regulation (6-fold) in
502 *aes*. Moreover, the higher accumulation of K^+ in *of* and the reduction level of this ion in *aes*, it
503 might also be related to the enhanced/reduced expression level of a TPK/KCO genes, respectively.
504 In fact, ectopic expression of a *P. euphratica* TPK1 in tobacco BY-2 cells have been reported to
505 improve salt tolerance, and reduce K^+ losses in transgenic cells compared to wild-type (Wang et
506 al., 2013). Thus, the increased shoot K^+ concentration and the improved salinity tolerance
507 identified in of might be related to its ability to control intracellular K^+ homeostasis. Very little
508 information is available about the role and functions of plant KEA transporters. Recent studies
509 reported the key role of KEA genes in the adaptation to environmental conditions. A KEA3 is
510 critical for high photosynthetic efficiency under fluctuating light (Armbruster et al., 2014) and
511 another KEA gene played important roles in drought tolerance of rice (Sheng et al., 2014). We
512 found a differential regulation of three KEA genes one of which was highly induced in *of* and the
513 others two repressed, which possibly contribute to salinity tolerance mechanisms. NHXs activity is
514 crucial for plant salt tolerance (Apse et al., 1999; Bassil et al., 2011). Unlike the other Arabidopsis
515 NHX isoforms, which are vacuolar, NHX6 is localized in endosomal compartments and in *aes* was
516 down-regulated, suggesting an impairment of homeostasis in endosomal compartments, which
517 could contribute to the greater salt sensitivity of this mutant.

518 Two member of anion channel families, SLAC1/SLAH3 (Vahisalu et al., 2008) and ALMT/QUAC1
519 (Sasaki et al., 2010) were differentially regulated in the two mutants under salt stress. These genes
520 are expressed in guard cells and mediate respectively Slow- and Rapid-type anion flow (Hedrich,
521 2012), and are involved in the stomatal response to various factors, including ABA, ozone, calcium,
522 salt, NO and light/dark transitions and water deficit (Wilkinson et al., 2012; Osakabe et al., 2014;
523 Vainonen and Kangasjärvi, 2015). In our study, the transcriptional induction of SLAH in *of* and the
524 repression of ALMT2 in *aes* under salt it might be coordinated respectively, by ABA changes and by
525 an alternate signaling pathway which causes stomatal guard cells to lose their sensitivity to ABA
526 (Fig 2e-d). This opposing transcriptional regulation in the mechanisms of stomatal aperture of the
527 two mutants directed our investigations to explore the signaling network executed by changes in
528 hormone biosynthesis which affected the reduction/increase in stomatal sensitivity to salt stress.
529 Thus, we speculated that *aes* plants were insensitive to ABA because of a consistently high ROS
530 stressful condition. This hypothesis is supported by the induction of ROS-Generating Oxidase such
531 as NOX3 and RBOH (Table S3; contig_34677 and contig_16549, respectively) and the repression of
532 H-type thioredoxin (THXhs), which in rice, regulated the redox-state of the apoplast under adverse
533 conditions (Zhang et al., 2011b).

534 4.3. ABA and ethylene signaling pathways and their interactions

535 The resilience of plants is largely dependent on the modulation of their hormone signaling
536 pathways (Peleg and Blumwald, 2011; Clays and Inzì, 2013). ABA plays significant roles in a number

of physiological processes and stress, including salinity responses (Osakabe et al., 2014). In the tolerant mutant, the increase in ABA levels can switch on the downstream modules likely CDPKs and SNF1-like related kinase which activates transcriptionally the anion channel SLAH1-like to release anions and close the stomata (Fig. 7), and this is might be reflected by the strongly reduction of CO_2 fixation after 6h and 3d (Fig. 2e, f). Moreover, ABA increase, prompts the induction of genes encoding osmoprotectans such as the LEA and THXh proteins (Table S12). In contrast, the less salt tolerance of *aes* might be related to a reduced ABA stomatal sensitivity as shown by the stomata that remain mostly open among the salt exposure (Fig. 2e, f). In fact, the perturbation in salinity-triggered calcium-dependent waves, can de-activated ABA signaling pathways and its synthesis, by both the down-regulation of the R-type anion channel ALMT2 and its precursor transcripts (Fig. 7).

Ethylene is also involved in the regulation of plant salt tolerance (Lei et al., 2011; Zhang et al., 2012; Jiang et al., 2013). The ethylene production was enhanced by salt in both mutants and after 3d shown a reduction only in *aes* (Fig. 2d), despite the biosynthetic transcriptional network at this time-point still remain induced with five ACS gene up-regulated. There is probably a direct and rapid mechanism to change ethylene production. In fact, a closer look at the ethylene signaling pathway genes highlighted an ETHYLENE OVERPRODUCER1 (ETO1; contig_45603) induced nearly 7-fold at 3d in *aes*. The ETO1 genes encodes for CULLIN3 E3 ubiquitin ligases which recognize and directly interact with ACS proteins targeting them for rapid degradation via 26S proteasome (Wang et al., 2004). Thus, it reasonable suggest the activation of post-translational regulation of ACS proteins. More interesting the lack of ETO1 function promotes soil-salinity tolerance in Arabidopsis mutants by a mechanism involving the strongly up-regulation of high-affinity K^+ transporter HAT5 gene, which enhanced the K^+ tissue accumulation (Jiang et al., 2013). Thus, in the mutants their opposite salinity sensitivity may be provided also by the differential transcriptional regulation of ETO1 and HAT5 genes, upregulated respectively in *aes* and *of* (Table S3; HAT5 contig_12124), which link their ethylene production and their retention of tissue K concentrations.

As recently has been reviewed in Müller and Munné-Bosch (2015), ERFs are key regulators in abiotic stress tolerance in several species. In our study, the transcriptome analysis identified 46 members of the AP2/ERF superfamily, differentially regulated upon NaCl stress (Table S7; Figure S11). Among these transcriptional activators/repressors, an ERF5 was differentially expressed between the mutants, downregulated in *of* and upregulated in *aes*. This TF has been reported to be a master regulators of leaf growth inhibition upon osmotic and salt stress (Dubois et al., 2013). Plants when exposed to salt stress, produce ethylene and the hormone further activates the signaling pathway involving ERFs, by the regulator NEK6, a kinase transcriptionally induced by ethylene and by salt stress (Skirycz et al., 2011a; Zhang et al., 2011). NEK6 could represent the intermediate regulator in the molecular mechanisms which involved salt and osmotic response via ethylene signaling (Dubois et al., 2013). It is possible that the activation of NEK6 in *of* allows the inhibition of ERF5, which was found to be downregulated in the tolerant mutant. We further speculated that this condition allow the activation of genes conferring a higher tolerance to sodium toxicity, which are not activated by ERF5 as already suggested by Dubois et al. (2013).
The ABA and ethylene interplay in salinity response through ERFs represent an important mechanism controlling stress-susceptibility traits (Cheng et al., 2013). The overexpression of ERF4 in Arabidopsis has been reported to repress the expression of ABA responsive genes, making the mutant less sensitive to ABA and hypersensitive to NaCl (Yang et al., 2005). Similarly, a transcript encoding for an ERF4 TF was upregulated under NaCl exposure and the expression of the ABA

responsive genes, rab11D, rab1-like and DREB1 (Table S3), was decreased in the *aes* sensitive mutant. These findings support our hypothesis regarding a putative de-activation in ABA signaling pathways which leads to increase salt susceptibility in *aes*.

5. Conclusion

In conclusion, we studied the complex salinity trigged events in term of a two-mode models: survival versus death. It is clear that there are different mechanisms of salinity tolerance acting in snapdragon when exposed to NaCl stress and the combination of them allows the plants survival.

(i) The osmotic tolerance signaling mechanisms activate shoot growth reduction through a better integration and transduction of environmental cues into growth programs. The regulator of cell cycle progression were transcriptionally reprogrammed to help in shaping and adapting plants under NaCl stess.

(ii) The modulation of calcium fluxes guided the reprogramming of the components of calcium signaling, such as Ca^{2+} channel and Ca^{2+} sensors, that are pivotal to modulate Na^{+} and K^{+} transporters which affect salinity tolerance traits tissue tolerance and anion exclusion;

(iii) The action of ABA and ethylene as a positive regulators of salt acclimation was effective by the activation of their biosynthesis and signaling transduction pathways.

Accession Number

Raw sequencing data (fastq files) were deposited in the Sequence Read Archive (SRA) at the NCBI (SRP071159).

Acknowledgements

We thank Prof. Alberto Pardossi of University of Pisa for his critical reading and contributions to the manuscript. This research was supported by PRIN2009BW3KL4 grant from MIUR, Italy.

REFERENCES

Aprile A, Mastrangelo AM, De Leonardis AM, Galiba G, Roncaglia E, Ferrari F, De Bellis L, Turchi L, Giuliano G, Cattivelli , 2009. Transcriptional profiling in response to terminal drought stress reveals differential responses along the wheat genome. BMC Genomics. 24; 10:279.

Apse MP, Aharon GS, Snedden WA, Blumwald E , 1999. Salt tolerance conferred by overexpression of a vacuolar Na+ /H+ antiport in Arabidopsis. Science 285:1256–1258.

Armbruster, U., Carrillo, LR., Venema, K., Pavlovic, L., Schmidtmann, E., Kornfeld, A., Jahns, P., Berry, JA., Kramer, DM., Jonikas, MC. , 2014. Ion antiport accelerates photosynthetic acclimation in fluctuating light environments. Nat Commun. 13;5:5439

Aversano, R., Contaldi, F., Ercolano, MR., Grosso, V., Iorizzo, M., Tatino, F., Xumerle, L., Dal Molin, A., Avanzato, C., Ferrarini, A., Delledonne, M., Sanseverino, W., Cigliano, RA., Capella-Gutierrez, S., Gabaldón, T., Frusciante, .1, Bradeen, JM., Carputo, D. , 2015. The Solanum commersonii Genome

617 Sequence Provides Insights into Adaptation to Stress Conditions and Genome Evolution of Wild
618 Potato Relatives. Plant Cell 27, 954-68.

619 Baena-González, E., Rolland, F., Thevelein, JM., Sheen, J. 2007 A central integrator of transcription
620 networks in plant stress and energy signalling. Nature 23, 938-42.

621 Barrero, J.M. et al. , 2006. Both abscisic acid , ABA.-dependent and ABA-independent pathways
622 govern the induction of NCED3, AAO3 and ABA1 in response to salt stress. Plant Cell Environ. 29,
623 2000–2008

624 Bassil E, Ohto MA, Esumi T, Tajima H, Zhu Z, Cagnac O, Belmonte M, Peleg Z, Yamaguchi T,
625 Blumwald E , 2011. The Arabidopsis intracellular Na+ /H+ antiporters NHX5 and NHX6 are
626 endosome associated and necessary for plant growth and development. Plant Cell 23:224–239

627 Battaglia M., Olvera-Carrillo Y., Garciarrubio A., Campos F. & Covarrubias A.A. , 2008. The
628 enigmatic LEA proteins and other hydrophilins. Plant Phys 148, 6–24.

629 Benjamini Y, Yekutieli D , 2001. The control of the false discovery rate in multiple testing under
630 dependency. Ann Stat 29:1165–1188.

631 Blumwald, E., Aharon, G.S. and Apse, M.P. , 2000. Sodium transport in plant cells. Biochim.
632 Biophys. Acta 1465, 140–151.

633 Boucher, V., Buitink, J., Lin, X., Boudet, B., Hoekstra, FA., Hundertmark, M., Renard, D., Leprince,
634 O., 2010. MtPM25 is an atypical hydrophobic late embryogenesis abundant protein that
635 dissociates cold and desiccation-aggregated proteins. Plant Cell Env. 33, 418–430.

636 Burke, G. R. and Strand, M. R. , 2012.. Deep sequencing identifies viral and wasp genes with
637 potential roles in replication of Microplitis demolitor Bracovirus. J Virol, 86, 3293-3306.

638 Chanroj, S., Wang, G., Venema, K., Zhang, MW., Delwiche, CF., Sze, H. , 2012.. Conserved and
639 diversified gene families of monovalent cation/H+ antiporters from algae to flowering plants.
640 Front. Plant Sci. 3, 1–18

641 Chen TW, Gan RCR, Wu TH, Huang Pj, Lee CY, et al. , 2012. FastAnnotator: an efficient transcript
642 annotation web tool. BMC Gen , Suppl 7.: S9, doi:10.1186/1471-2164-13-S7-S9

643 Cheng, M.C., Liao, P.M., Kuo, W.W., Lin, T.P., 2013. The Arabidopsis ETHYLENE RESPONSE FACTOR1
644 regulates abiotic stress-responsive gene expression by binding to different cis-acting elements in
645 response to different stress signals. Plant Physiol ,162, 1566–1582

646 Claeys, H., Skirycz, A., Maleux, K., Inze´, D. , 2012. DELLA signaling mediates stress-induced cell
647 differentiation in Arabidopsis leaves through modulation of APC/C activity. Plant Physiol 2012,
648 159, 739-747.

649 Claeys, H., Inzé, D. , 2013. The Agony of Choice: How Plants Balance Growth and Survival under
650 Water-Limiting Conditions. Plant Phys, 162, 1768–1779.

651 Claeys, H., Van Landeghem, S., Dubois, M., Maleux, K., Inzé, D., 2014. What Is Stress? Dose-
652 Response Effects in Commonly Used in Vitro Stress Assays. Plant Physiol 165, 519–527.

653 Cools, T., Veylder, L.D., 2009. DNA stress checkpoint control and plant development. Current
654 Opinion in Plant Biology, 12, 23–28.

655 Cosgrove, DJ. , 2005. Growth of the plant cell wall. Nat Rev Mol Cell Biol 6: 850–861

656 Cuin TA, Betts SA, Chalmandrier R, Shabala S , 2008. A root's ability to retain K+ correlates with salt
657 tolerance in wheat. J Exp Bot 59: 2697–2706

658 Cuin TA, Miller AJ, Laurie SA, Leigh RA , 2003. Potassium activities in cell compartments of salt-
659 grown barley leaves. J Exp Bot 54:657–661

660 De Angeli, A., Monachello, D., Ephritikhine, G., Frachisse, JM., Thomine, S., Gambale, F., Barbier-
661 Brygoo, H. 2006. The nitrate/proton antiporter AtCLCa mediates nitrate accumulation in plant
662 vacuoles. Nature. 2006 24, 939-42.

663 Deinlein, U., Stephan, A.B., Horie, T., Luo, W., Xu, G. and Schroeder, J.I. , 2014. Plant salt-tolerance
664 mechanisms. Trends Plant Sci. 19, 371–379.

665 Diedhiou, CJ., Golldack, D. , 2006. Salt-dependent regulation of chloride channel transcripts in rice.
666 Plant Sci 170:793–800

667 Dinneny, JR, 2015 Traversing organizational scales in plant salt-stress responses. Curr Opin Plant
668 Biol 23, 70–75

669 Dong, W. et al. , 2013. Wheat oxophytodienoate reductase gene TaOPR1 confers salinity tolerance
670 via enhancement of abscisic acid signaling and reactive oxygen species scavenging. Plant Physiol.
671 161, 1217–1228

672 Du Z, Zhou X, Ling Y, Zhang Z, Su Z. , 2010. agriGO: a GO analysis toolkit for the agricultural
673 community. Nucleic Acids Research 38: W64-W70.

674 Dubois, M., Skirycz, A., Claeys, H., Maleux, K., Dhondt, S., De Bodt, S., VandenBossche, R., De
675 Milde, L., Yoshizumi, T., Matsui, M., et al (2013) ETHYLENE RESPONSE FACTOR6 acts as a central
676 regulator of leaf growth under waterlimiting conditions in Arabidopsis. Plant Physiol 162, 319–332

677 Dugas DV, Monaco MK, Olsen A, Klein RR, Kumari S, Ware D, Klein PE. , 2011. Functional
678 annotation of the transcriptome of Sorghum bicolor in response to osmotic stress and abscisic
679 acid. BMC Genomics. 18; 12:514

680 Ferrante, A., Trivellini, A., Malorgio, F., Carmassi, G., Vernieri, P., Serra, G. 2011. Effect of seawater
681 aerosol on leaves of six plant species potentially useful for ornamental purposes in coastal areas.
682 Scientia Horticulturae 128, 332–341.

683 Flagella, Z., Trono, D., Pompa M., Di Fonzo, N., Pastore D. , 2006. Seawater stress applied at
684 germination affects mitochondrial function in durum wheat , Triticum durum. early seedlings.
685 Funct. Plant Biol. 33, 357–366

686 Flowers,T.J, Munns R., Colmer TD., 2015 Sodium chloride toxicity and the cellular basis of salt
687 tolerance in halophytes. Annals of Botany 115: 419-431.Geng,Y., Wu, R., Wee, CW., Xie, F., Wei, X.,
688 Chan, PMY., Tham, C., Duan, L., Dinnenya JR. , 2013. A Spatio-Temporal Understanding of Growth
689 Regulation during the Salt Stress Response in Arabidopsis. Plant Cell, 25, 2132–2154.

690 Guo, J., Shi, G., Guo, X., Zhang, L., Xu, W., Wang, Y., Su, Z., Hua, J. , 2015. Transcriptome analysis
691 reveals that distinct metabolic pathways operate in salt-tolerant and salt-sensitive upland cotton
692 varieties subjected to salinity stress. Plant Sci. 238, 33-45.

693 Gwinn, D.M., Shackelford, D.B., Egan, D.F., Mihaylova, M.M., Mery, A., Vasquez, D.S., Turk, B.E.,
694 Shaw R.J , 2008. AMPK phosphorylation of raptor mediates a metabolic checkpoint Mol. Cell, 30,
695 214–226.

696 Han, X., Tang, S., An, Y., Zheng, DC., Xia, XL., Yin, WL. , 2013. Overexpression of the poplar NF-YB7
697 transcription factor confers drought tolerance and improves water-use efficiency in Arabidopsis. J
698 Exp Bot. 64, 4589-601.

699 Hashimoto, M., Negi, J., Young, J., Israelsson, M., Schroeder, J. I. & Iba, K. 2006 Arabidopsis HT1
700 kinase controls stomatal movements in response to CO2. Nat. Cell Biol. 8, 391–397.

701 Hedrich, R. 2012. Ion channels in plants. Physiol Rev., 92, 1777-811.

702 Iqbal, N., Umara, S., Khan, N.A., Iqbal, M., Khan, R., , 2014. A new perspective of phytohormones in
703 salinity tolerance: Regulation of proline metabolism. Environmental and Experimental Botany 100,
704 34– 42;

705 Ismail A, Seo M, Takebayashi Y, Kamiya Y, Eiche E, Nick P. , 2014.. Salt adaptation requires
706 suppression of jasmonate signaling. Protoplasma doi.10.1007/s00709-013-0591-y.

707 Ismail, A., Takeda, S., Nick, P. , 2014. Life and death under salt stress: same players, different
708 timing? 65 J EXP Bot. 12, 2963-2979.

709 Jacoby, RP., Taylor, NL., Millar, AH., , 2011. The role of mitochondrial respiration in salinity
710 tolerance. Trends Plant Sci 16, 11

711 Juraniec, M., Heyman, J., Schubert, V., Salis, P., De Veylder, L., Verbruggen, N. , 2016. Arabidopsis
712 COPPER MODIFIED RESISTANCE1/PATRONUS1 is essential for growth adaptation to stress and
713 required for mitotic onset control. New Phyt 209, 177–191.

714 Julkowska, MM., Testerink, C. , 2015. Tuning plant signaling and growth to survive salt. Trends
715 Plant Sci, Vol. 20, No. 9

716 Julkowska M.M.1, Klei K., Fokkens L., Haring M.A., Schranz M.E. & Testerink C. , 2016. Natural
717 variation in rosette size under salt stress conditions corresponds to developmental differences
718 between Arabidopsis accessions and allelic variation in the LRR-KISS gene. Journal of Experimental
719 Botany, doi:10.1093/jxb/erw015

720 Kasai, K., Fukayama, H., Uchida, N., Mori, N., Yasuda, T., Oji, Y., Nakamura, C. , 1998. Salinity
721 tolerance in Triticum aestivum, Lophopyrum elongatum amphiploid and 5E disomic addition line
722 evaluated by NaCl effects on photosynthesis and respiration. Cereal Res. Commun. 26, 281–287.

723 Kiferle, C., Lucchesini, M., Maggini, R., Pardossi, A., Mensuali-Sodi, A. , 2014. In vitro culture of
724 sweet basil: gas exchanges, growth, and rosmarinic acid production. Biologia Plantarum 58: 601-
725 610.

726 Kitsios, G., Doonan, JH. , 2011. Cyclin dependent protein kinases and stress responses in plants.
727 Plant Signal Behav. 6, 204–209.

728 Krasensky J., Jonak C. , 2012. Drought, salt, and temperature stress-induced metabolic
729 rearrangements and regulatory networks J Exp Bot 63, 1593–1608.

730 Lehti-Shiu MD, Shiu SH , 2012. Diversity, classification and function of the plant protein kinase
731 superfamily. Phil. Trans. R. Soc. B, 367, 2619–2639

732 Lehti-Shiu, MD., Shiu, SH. 2012 Diversity, classification and function of the plant protein kinase
733 superfamily. Philos Trans R Soc Lond B Biol Sci. 19;367, 2619-39.

734 Lei, G., Shen, M., Li, Z.G., Zhang, B., Duan, K.X., Wang, N., Cao, Y.R., Zhang, W.K.,Ma, B., Ling, H.Q.,
735 Chen, S.Y., and Zhang, J.S. , 2011.. EIN2 regulates salt stress response and interacts with a MA3
736 domain-containing protein ECIP1 in Arabidopsis. Plant Cell Environ. 34: 1678–1692.

737 Luan S1 2009 The CBL-CIPK network in plant calcium signaling. Trends Plant Sci. 14, 37-42.

738 Ma, X., Zhu, X., Li, C., Song, Y., Zhang, W., Xia, G., Wang, M.. , 2015. Overexpression of wheat NF-
739 YA10 gene regulates the salinity stress response in Arabidopsis thaliana. Plant Physiol Biochem. 86,
740 34-43.

741 Maathuis, FJM. , 2014. Sodium in plants: perception, signalling, and regulation of sodium fluxes. J
742 Exp Bot 65, 849–858.

743 Mortazavi, A., Williams, B. A., McCue, K., Schaeffer L. and Wold B. , 2008.. Mapping and
744 quantifying mammalian transcriptomes by RNA-Seq. Nat. Methods, 5, 621-628.

745 Müller, M., Munné-Bosch, S., 2015. Ethylene Response Factors: A Key Regulatory Hub in Hormone
746 and Stress Signaling. Plant Physiol., 169, 32-41.

747 Munns, R. , 2002. Comparative physiology of salt and water stress. Plant Cell Environ. 25, 239–250.

748 Munns, R.,Tester M. , 2008. Mechanisms of salinity tolerance. Annu. Rev. Plant Biol 59, 651-681

749 Munns, R., and Tester, M. , 2008. Mechanisms of salinity tolerance. Annu. Rev. Plant Biol. **59**, 651–
750 681.

751 Munns, R., 2010. Approaches to Identifying Genes for Salinity Tolerance and the Importance of
752 Timescale. In: Plant Stress Tolerance, Methods and Protocols, Edited By Sunkar R., Humana Press,
753 Springer New York, pages 25-38.

754 Nicot, N., Hausman, JF., Hoffmann, L., Evers, D. , 2005. Housekeeping gene selection for real-time
755 RT-PCR normalization in potato during biotic and abiotic stress. J Exp Bot. 56, 2907-14.

756 Nietzsche, M., Landgrafa, R., Tohgeb, T., Börnkea, F , 2016. A protein–protein interaction network
757 linking the energy-sensor kinase SnRK1 to multiple signaling pathways in Arabidopsis thaliana.Curr
758 Opin Plant Biol, doi:10.1016/j.cpb.2015.10.004.

759 Ng, S., Giraud, E., Duncan, O., Law, SR., Wang, Y., Xu, L., Narsai, R., Carrie, C., Walker, H., Day, DA.,
760 Blanco, NE., Strand, Å., Whelan, J., Ivanova, A. 2013 Cyclin-dependent kinase E1 , CDKE1. provides
761 a cellular switch in plants between growth and stress responses. J Biol Chem. 288, 3449-59

762 Omidbakhshfard, MA., Proost, S., Fujikura, U., Mueller-Roeber, B. , 2015. Growth-Regulating
763 Factors , GRFs.: A Small Transcription Factor Family with Important Functions in Plant Biology. Mol
764 Plant. 6, 998-1010.

765 O'Rourke, J. A., Yang, S. S. Miller, S. S., Bucciarelli, B., Liu, J., Rydeen, A., Bozsoki, Z., Uhde-Stone,
766 C., Tu, Z. J., Allan, D., Gronwald J. W. and Vance C. P. , 2013.. An RNA-Seq transcriptome analysis of
767 orthophosphate-deficient white lupin reveals novel insights into phosphorus acclimation in plants.
768 Plant Physiol, 161, 705-724.

769 Orsini F, Cascone P, De Pascale S, Barbieri G, Corrado G, Rao R, Maggio A. , 2010. Systemin-
770 dependent salinity tolerance in tomato: evidence of specific convergence of abiotic and biotic
771 stress responses. Physiol Plant. 138, 10-21.

772 Osakabe, Y., Yamaguchi-Shinozaki, K., Shinozaki, K, Phan Tran, L. S. , 2013.. Sensing the
773 environment: key roles of membrane-localized kinases in plant perception and response to abiotic
774 stress. J. Exp. Bot. 64 445–458 10.1093/jxb/ers354

775 Osakabe, Y., Yamaguchi-Shinozaki, K., Shinozaki, K., Tran, LS. , 2014. ABA control of plant
776 macroelement membrane transport systems in response to water deficit and high salinity. New
777 Phytol. 202, 35-49.

778 Quereda, V., Porlan, E., Cañamero, M., Dubus, P., Malumbres, M. 2016. An essential role for Ink4
779 and Cip/Kip cell-cycle inhibitors in preventing replicative stress. Cell Death & Differentiation 23,
780 430-441.

781 Palmeros-Suárez, PA., Massange-Sánchez, JA., Martínez-Gallardo, NA., Montero-Vargas, JM.,
782 Gómez-Leyva, JF., Délano-Frier, JP. , 2015. The overexpression of an Amaranthus hypochondriacus
783 NF-YC gene modifies growth and confers water deficit stress resistance in Arabidopsis. Plant Sci.
784 240, 25-40.

785 Polyn, S., Willems, A., Veylder, L.D., 2015. Cell cycle entry, maintenance, and exit during plant
786 development. Current Opinion in Plant Biology, 23, 1–7.

787 Pandey, GK., Kanwar, P., Singh, A., Steinhorst, L., Pandey, A., Yadav, AK., Tokas, I., Sanyal, SK., Kim,
788 BG., Lee, SC., Cheong, YH., Kudla, J., Luan, S. 2015 Calcineurin B-Like Protein-Interacting Protein
789 Kinase CIPK21 Regulates Osmotic and Salt Stress Responses in Arabidopsis. Plant Physiol. 169, 780-
790 92

791 Peleg Z. & Blumwald E. , 2011. Hormone balance and abiotic stress tolerance in crop plants.
792 Current Opinion in Plant Biology **14**, 1–6;

793 Peng, Z., He, S., Gong, W., Sun, J., Pan, Z., Xu, F., Lu, Y., Du, X. , 2014. Comprehensive analysis of
794 differentially expressed genes and transcriptional regulation induced by salt stress in two
795 contrasting cotton genotypes. BMC Genomics 15: 760

796 Petroni, K., Kumimoto, RW., Gnesutta, N., Calvenzani, V., Fornari, M., Tonelli, C., Holt, BF.,
797 Mantovani, R. , 2012. The promiscuous life of plant NUCLEAR FACTOR Y transcription factors. Plant
798 Cell 24, 4777-92

Qi, X., Li, MW., Xie, M., Liu, X., Ni, M., Shao, G., Song, C., Kay-Yuen, Yim A., Tao ,Y., Wong, FL., Isobe, S., Wong, CF., Wong, KS., Xu, C., Li, C., Wang, Y., Guan, R., Sun, F., Fan, G., Xiao, Z., Zhou, F., Phang, TH., Liu, X., Tong, SW., Chan, TF., Yiu, SM., Tabata, S., Wang, J., Xu, X., Lam, HM. , 2014. Identification of a novel salt tolerance gene in wild soybean by whole-genome sequencing. Nat Commun. 9;5:4340.

Qiu QS, Guo Y, Quintero FJ, Pardo JM, Schumaker KS, Zhu JK , 2004. Regulation of vacuolar Na+/H+ exchange in Arabidopsis thaliana by the salt-overly-sensitive , SOS. pathway. J Biol Chem. 2, 207-15.

Radziejwoski A, Vlieghe K, Lammens T, Berckmans B, Maes S, Jansen MAK, Knappe, K., Albert, A., Seidlitz H.K., Bahnweg, G., Inze´ D., De Veylder, L. , 2011. Atypical E2F activity coordinates PHR1 photolyase gene transcription with endoreduplication onset. EMBO J, 30, 355-363.

Reddy NRR,Mehta RH, Soni PH, Makasana J, Gajbhiye NA, Ponnuchamy M, Kumar J., , 2015. Next Generation Sequencing and Transcriptome Analysis Predicts Biosynthetic Pathway of Sennosides from Senna , Cassia angustifolia Vahl.., a Non-Model Plant with Potent Laxative Properties. PLoS One. 2015; 10, 6.: e0129422.

Repka V, Fischerová I, Šilhárová K. , 2004. Methyl jasmonate is a potent elicitor of multiple defense responses in grapevine leaves and cellsuspension cultures. Biologia Plant 48, 273–283.

Roy S.J., Negrao S. & Tester M. , 2014. Salt resistant crop plants. Curr Opin Plant Biotech 26:115–124.

Rymen, B., Sugimoto, K. , 2012. Tuning growth to the environmental demands. Curr Opin Plant Biol, 15, 683–690.

Sánchez-Barrena MJ, Martínez-Ripoll M, Zhu JK, Albert A , 2005. The structure of the Arabidopsis thaliana SOS3: molecular mechanism of sensing calcium for salt stress response. J Mol Biol. 2005 Feb 4; 345, 5.:1253-64.

Sasaki, T., Mori, IC., Furuichi, T., Munemasa, S., Toyooka, K., Matsuoka, K., Murata, Y., Yamamoto, Y. 2010. Closing plant stomata requires a homolog of an aluminum-activated malate transporter. Plant and Cell Physiology 51: 354–365.

Schoenfelder, K.P., Fox, D.T. 2014. The expanding implications of polyploidy. J Cell Biol, 209, 485-491.

Scholesemail, D.R., Paige, K.N., 2015. Plasticity in ploidy: a generalized response to stress. Trends Plant Sci, 20, 165–175.

Schmöckel, SM., Garcia, AF., Berger, B., Tester, M., Webb, AA., Roy, SJ. 2015 Different NaCl-induced calcium signatures in the Arabidopsis thaliana ecotypes Col-0 and C24. PLoS One. 2015 Feb 27;10, 2.:e0117564.

Schwarz-Sommer, Z., Davies, B., Hudson, A., 2003. An everlasting pioneer: the story of Antirrhinum research. Nature Reviews, 4, 655-664.

Skirycz, A., Claeys, H., De Bodt, S., Oikawa, A., Shinoda, S., Andriankaja, M., Maleux, K., Eloy, N.B., Coppens, F., Yoo, S.-D., et al. 2011. Pause-and-stop: the effects of osmotic stress on cell

837 proliferation during early leaf development in Arabidopsis and a role for ethylene signaling in cell
838 cycle arrest. Plant Cell 23, 1876–1888

839 Shabalaa, S., Pottosina, I. , 2014. Regulation of potassium transport in plants under hostile
840 conditions: implications for abiotic and biotic stress tolerance. Physiologia Plant 151: 257–279.
841 2014

842 Sheng P, Tan J, Jin M, Wu F, Zhou K, Ma W, Heng Y, Wang J, Guo X, Zhang X, Cheng Z, Liu L, Wang
843 C, Liu X, Wan J. , 2014. Albino midrib 1, encoding a putative potassium efflux antiporter, affects
844 chloroplast development and drought tolerance in rice. Plant Cell Rep., 33, 9.:1581-94

845 Sheng, P., Tan, J., Jin, M., Wu, F., Zhou, K., Ma, W., Heng, Y., Wang, J., Guo, X., Zhang, X., Cheng, Z.,
846 Liu, L., Wang, C., Liu X, Wan J. , 2014. Albino midrib 1, encoding a putative potassium efflux
847 antiporter, affects chloroplast development and drought tolerance in rice. Plant Cell Rep. 33,
848 1581-94.

849 Sun, X., Li, J. , 2013. pairheatmap: Comparing expression profiles of gene groups in heatmaps,
850 Computer Methods and Programs in Biomedicine, 112: 599-606.

851 Swarbreck, SM., Colaço, R., Davies, JM. 2013 Plant calcium-permeable channels. Plant Physiol. 163,
852 514-22. Torres, MA., Dangl, JL., Jones, JDG. , 2002. Arabidopsis gp91phox homologues AtrbohD
853 and AtrbohF are required for accumulation of reactive oxygen intermediates in the plant defense
854 response. Proc Natl Acad Sci U S A 2002, 99:517-522.

855 Trivellini, A., Ferrante, A., Vernieri, P., Serra, G. 2011. Effects of abscisic acid on ethylene
856 biosynthesis and perception in Hibiscus rosasinensis L. flower development. J Exp Bot, 62, 5437–
857 5452

858 Trivellini, A., Jibran, R., Watson, LM., O'Donoghue, EM., Ferrante, A., Sullivan, KL., Dijkwel, PP.,
859 Hunter, DA , 2012. Carbon deprivation-driven transcriptome reprogramming in detached
860 developmentally arresting Arabidopsis inflorescences. Plant Physiology 160, 1357–1372

861 Vahisalu, T., Kollist T., Wang Y.F., Nishimura N., Chan, N-W., Valerio, G., Lamminmäki, A., Brosché,
862 M., Moldau, H., Desikan, R., Schroeder, J.L., Kangasjärvi J., , 2008. SLAC1 is required for plant guard
863 cell S-type anion channel function in stomatal signaling. Nature 452, 487–491.

864 Vaidyanathan, H., Sivakumar, P., Chakrabarty, R., Thomas, G., , 2003. Scavenging of reactive
865 oxygen species in NaCl-stressed rice , Oryza sativa L.. differential response in salt-tolerant and
866 sensitive varieties. Plant Sci, 165, 1411–1418

867 Vainonen, JP., Kangasjärvi J. , 2015. Plant signalling in acute ozone exposure. Plant Cell Env. 38,
868 240–252

869 Vernieri, P., Perata, P., Armellini, D., Bugnoli, M., Presentini, R., Lorenzi, R., Ceccarelli, N., Alpi, A.,
870 Tognoni, F., 1989. Solid phase radioimmunoassay for the quantitation of abscisic acid in plant
871 crude extracts using a new monoclonal antibody. J. Plant Physiol. 134, 441–446.

872 Victoria, F. C., da Maia L. C. and de Oliveira, A. C. , 2011.. In silico comparative analysis of SSR
873 markers in plants. BMC Plant Biol, 11, 15-30.

874 Walia H, Wilson C, Ismail AM, Close TJ, Cui X , 2009. Comparing genomic expression patterns
875 across plant species reveals highly diverged transcriptional dynamics in response to salt stress.
876 BMC Genomics. 25; 10:398

877 Wang, F., Deng, S., Ding, M., Sun, J., Wang, M., Zhu, H., Han, Y., Shen, Z., Jing, X., Zhang, F., Hu, Y.,
878 Shen, X., Chen, S. , 2013. Overexpression of a poplar two-pore K+ channel enhances salinity
879 tolerance in tobacco cells. Plant Cell Tiss Organ Cult, 112:19–31.

880 Wang, KL., Yoshida, H., Lurin, C., Ecker, JR., , 2004. Regulation of ethylene gas biosynthesis by the
881 Arabidopsis ETO1 protein. Nature 2004, 428:945-950.

882 Wilkinson, S., Mills, G., Illidge, R., Davies, WJ., , 2012. How is ozone pollution reducing our food
883 supply? J Exp Bot. 63, 527–536.

884 Wilson, ME., Basu, MR., Bhaskara, GB., Verslues, PE., Haswell, ES. , 2014. Plastid osmotic stress
885 activates cellular stress responses in Arabidopsis. Plant Physiol. 165, 119-28.

886 Wu, J., Mao, X., Cai, T., Luo, J. & Wei, L. , 2006. KOBAS server: a web-based platform for
887 automated annotation and pathway identification. Nucleic Acids Res, 34, W720-724.

888 Wu, L., Zhang, Z., Zhang, H., Wang, X.C., and Huang, R. , 2008.. Transcriptional modulation of
889 ethylene response factor protein JERF3 in the oxidative stress response enhances tolerance of
890 tobacco seedlings to salt, drought, and freezing. Plant Physiol. 148, 1953–1963.

891 Xie C, Mao X, Huang J, Ding Y, Wu J, Dong S, Kong L, Gao G, Li CY, Wei L. , 2011. KOBAS 2.0: a web
892 server for annotation and identification of enriched pathways and diseases. Nucleic Acids Res.
893 2011;39:W316–W322.

894 Xiong, Y., McCormack, M.,. Li, L., Hall, Q., Xiang, C., Sheen, J. 2013. Glucose-TOR signalling
895 reprograms the transcriptome and activates meristems. Nature, 496, 181–186.

896 Yang, Z., Tian, L., Latoszek-Green, M., Brown, D., Wu, K. (2005) Arabidopsis ERF4 is a
897 transcriptional repressor capable of modulating ethylene and abscisic acid responses. Plant Mol
898 Biol 58: 585–596

899 Yi, D., Lessa Alvim Kamei, C., Cools, T., Vanderauwera, S., Takahashi, N., Okushima, Y., Eekhout, T.,
900 Okamoto Yoshiyama, K., Larkin, J., Van den Daele, H. 2014. The Arabidopsis Siamese-related cyclin-
901 dependent kinase inhibitors SMR5 and SMR7 regulate the DNA damage checkpoint in response to
902 reactive oxygen species Plant Cell, 26, 296–309.

903 Zhang L, Xing D. 2008. Methyl jasmonate induces production of reactive oxygen species and
904 alterations in mitochondrial dynamics that precede photosynthetic dysfunction and subsequent
905 cell death. Plant Cell Phys 49, 1092–1111.

906 Zhang, B., Chen, H-W., Mu, R-L., Zhang, W-K., Zhao, M-Y., Wei, W., Wang, F., Yu, H., Lei, G., Zou, H-
907 F., , 2011a. NIMA-related kinase NEK6 affects plant growth and stress response in Arabidopsis.
908 Plant J 68: 830–843

909 Zhang, CZ., Zhao, BC., Ge, WN., Zhang, YF., Song, Y., Sun, DH., Guo Y. , 2011b. An Apoplastic H-Type
910 Thioredoxin Is Involved in the Stress Response through Regulation of the Apoplastic Reactive
911 Oxygen Species in Rice. Plant Physiol. 157, 1884–1899.

912 Zhang, Z., Wang, J., Zhang, R., and Huang, R. , 2012.. The ethylene response factor AtERF98
913 enhances tolerance to salt through the transcriptional activation of ascorbic acid synthesis in
914 Arabidopsis. Plant J. 71: 273–287.

915 Zhu, J.K., , 2002. Salt and drought stress signal transduction in plants. Annu. Rev. Plant Biol. **53**,
916 247–273.

917

918 **Figure legends (979 words)**

919 **Figure 1.** Phenotypes of *of* and *aes* plants on MS agar with or without NaCl supplement.

920 (a) Relative shoot area and root length of seedlings after 1 week after root bending assay. Effect
921 on long-term exposure of 200mM NaCl of in-vitro growing shoot on water loss and growth
922 reduction. The values are expressed as percentage of control.

923 (b) Appearance of seedlings grown first on vertical MS agar plates for 5 days before being
924 transferred to vertical agar plates without (control) or with (100 mM and 300 mM) NaCl for 7 days.
925 The plates were placed upside down for root bending. The photographs were taken 1 week after
926 seedling transfer.

927 (c) Effect of long-term exposure of 200 mM NaCl (21 days) of in-vitro growing shoots on
928 chlorophyll and anthocyanins degradation expressed as a percentage of control.

929 Data were analyzed by Student's t-test. Data are means (n=5) ± SE. Different letters denote
930 significant differences at $P \leq 0.05$.

931 **Figure 2.** Sensitivity of *of* and *aes* shoots to short-term exposure (6h and 3d) of 200 mM NaCl
932 concentration.

933 (a) Appearance of shoots.

934 (b) 3days exposure of NaCl of in-vitro growing shoots on chlorophyll degradation expressed as a
935 percentage of control.

936 (c) Endogenous ABA content.

937 (d) Ethylene production.

938 (e) Net photosynthetic rate after 6h.

939 (f) Net photosynthetic rate after 3d.

940 All data were analyzed by ANOVA and differences between the mutants and treatments were
941 analysed by a Bonferroni posttest. The results shown are the means (n=5) ± SE. Different letters
942 denote significant differences at $P \leq 0.05$.

943 **Figure 3.** Na+ and K+, Ca2+ and Mg2+ contents in shoots of *of* and *aes* treated with 200 mM NaCl
944 for 3 days.

945 (a) Na^+, (b) K^+, (c) Ca^{2+}, (d) Mg^{2+} content in shoot.

All data were analyzed by ANOVA and differences between the mutants and treatments were analysed by a Bonferroni posttest. The results shown are the means ± SE of nine pooled shoots of three biological replicates. Different letters denote significant differences at $P \leq 0.05$.

Figure 4. Overview of RNA-seq-based transcriptome profiling of high salinity response in snapdragon shoots

(a) Contig length distribution showing by histogram of the length distribution of assembled contig.

(b) The BLAST top hit species taxonomic distribution from each transcript in de novo transcriptome assembly.

(c) Numbers of salt-responsive genes after 6 hours and 3 days of treatment exposure in MAM 7 and MAM 219 mutants. The comparisons were 219 control (ctrl) versus 219 200 mM - 6h (219-6h), 219 ctrl vs. 219 200 mM - 3d (219-3d), 7 ctrl versus 7 200 mM – 6h (7-6h) and 7 ctrl versus 200 mM – 3d (7-3d).

(d) Heat map illustrating expression profiles of 9,199 transcripts differentially expressed due to NaCl exposure (6h and 3d) in the two mutants (219 and 7) and the significantly enriched KEGG pathways associated with the cluster.in the clusters. Red indicates high expression, white indicates intermediate expression, and blue indicates low expression. See also Supplemental Tables S1 and S2.

(e) Multi-dimensional scaling (MDS) plot of gene expression of the 8 RNA-seq libraries.

Figure 5. Heat maps of salt stress effects on kinase family (a), transcription factor families (b) and transport systems (c) during the two time-points in of and aes. Data are from RNA-seq and are expressed as the log2 of fold change (salt, control). Red and blu indicate up-regulation and down-regulation, respectively. The number in the colored squares indicate the number of transcripts.

Figure 6. Simplified molecular working model for the shoots salinity response in case of tolerance (*of*) or sensitivity (*aes*).

SUPPORTING INFORMATION

Figure S1. Five-day-old snapdragon wild type seedlings with 1- to 2-cm-long roots, on vertical agar plates (A), were transferred to plates supplemented with NaCl (0, 50,100, 200 and 400) and allowed to grow upside down for 1 week (B) and for 2 weeks (C).

Figure S2. Functional annotation statistics. The number of blast hits including known and unknown protein function (A) is reported.

Figure S3. Functional annotation statistics. The number of sequences that contain the annotation in one or all of the three functional categories is reported. Gene Ontology (GO), Enzyme and Domain. A total of 26354 contigs were completely annotated by FastAnnotator.

Figure S4. Most highly represented GO-terms in the *Antirrhinum majus* transcriptome: biological process (a), cellular component (b), and molecular function (c) terms are represented. GO-terms annotation were assigned to each transcript using the Blast2GO pipeline.

Figure S5. Validation of differential gene expression results obtained by RNA-seq. Correlation of fold change analyzed by RNA-Seq platform (x axis) with data obtained using real-time PCR (y axis)

Figure S6. Heat maps of salt stress effects on kinase RLK families. Data are from RNA-seq and are expressed as the log2 of fold-change (salt, control). Red and blu indicate up-regulation and down-regulation, respectively. The number in the colored squares indicate the number of transcripts.

Table S1. List of snapdragon mutants screened using a root-bending assay at 100 and 300 mM NaCl. The 62 mutants were selected among more than 450 genotypes for their phenotype description provided by the snapdragon database, DragonDB (http://www.antirrhinum.net/).

Table S2. Phenotypic responses of snapdragon mutants to salinity stress (100mM and 200mM NaCl) after long-term exposure (21 days)

Table S3. All DETs in *of* and *aes*

Table S4. Primers used for qRT-PCR

Table S5. List of selected "sensory mechanisms" genes

Table S6. List of selected "transcriptional control" genes

Table S7. List of selected "cell proliferation and cell expansion" genes

Table S8. List of selected "network of Na and K transport process" genes

Table S9. List of selected "ABA signaling pathway" genes

Table S10. List of selected "Ethylene signaling pathway" genes

Table S11. List of selected "antioxidant and osmoprotectant" genes

Table S12. Supplementary information on RNA-seq data

1 **LIST OF FIGURES**

2 **Figure 1**

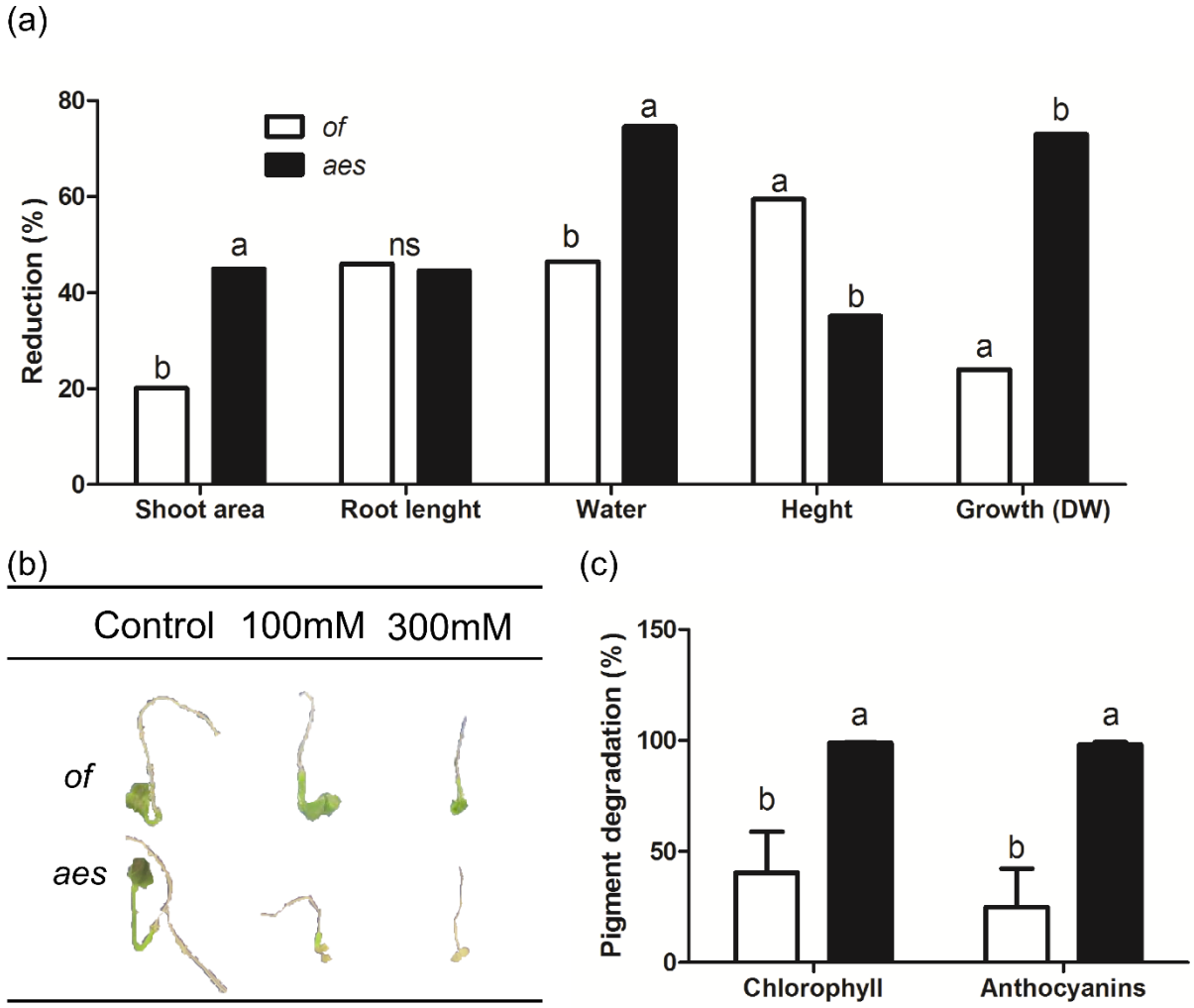

3

4

Figure 2.

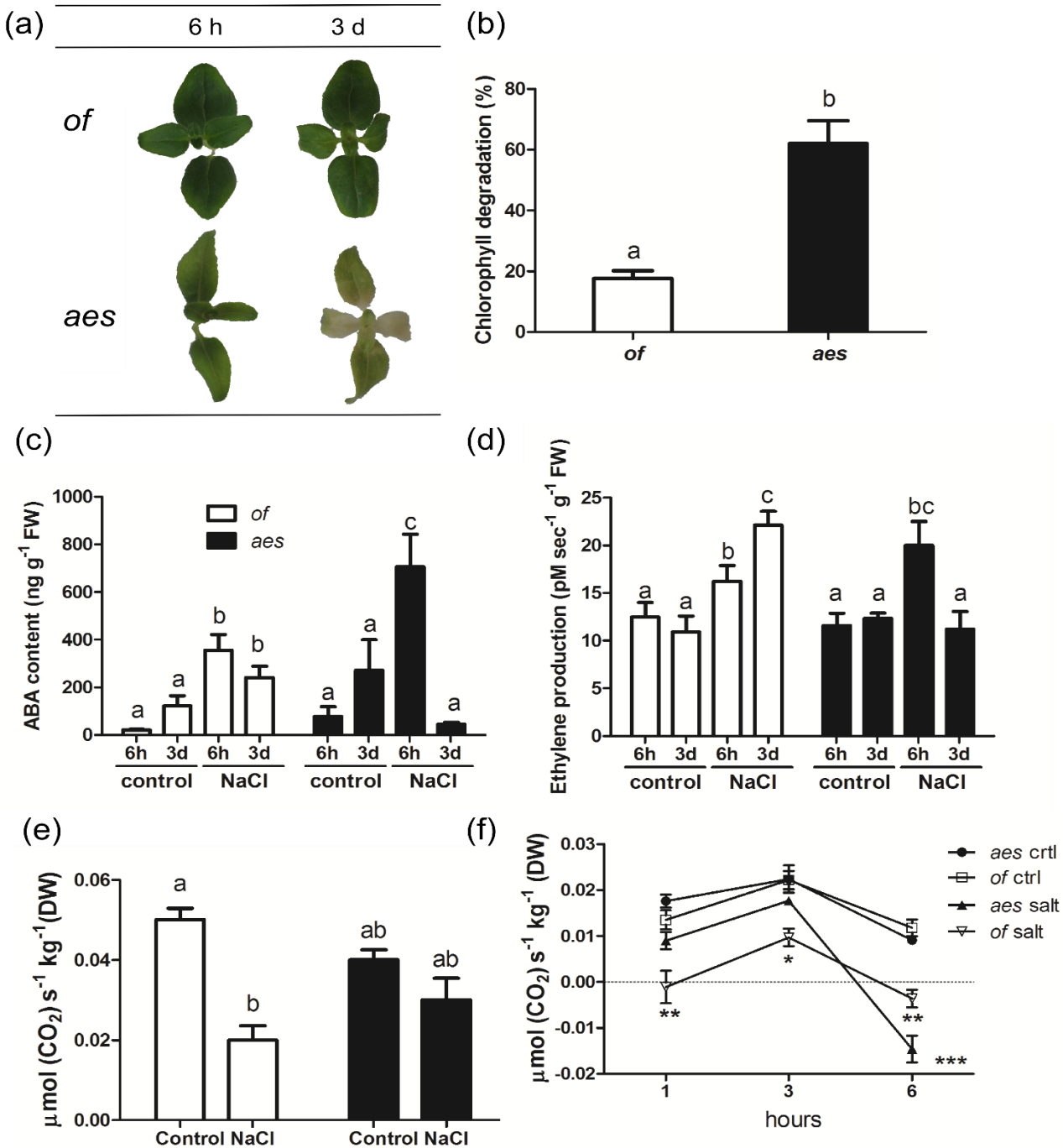
(a)
6 h
3 d
of
aes
(b)
Chlorophyll degradation (%)
80
60
40
20
0
a
b
of
aes
(c)
ABA content (ng g-1 FW)
1000
800
600
400
200
0
of
aes
a
a
b
b
a
a
c
a
6h
3d
6h
3d
6h
3d
6h
3d
control
NaCl
control
NaCl
(d)
Ethylene production (pM sec-1 g-1 FW)
25
20
15
10
5
0
a
a
b
c
a
a
bc
a
6h
3d
6h
3d
6h
3d
6h
3d
control
NaCl
control
NaCl
(e)
µmol (CO2) s-1 kg-1 (DW)
0.06
0.04
0.02
0.00
a
b
ab
ab
Control NaCl
Control NaCl
(f)
µmol (CO2) s-1 kg-1 (DW)
0.03
0.02
0.01
0.00
-0.01
-0.02
aes crtl
of ctrl
aes salt
of salt
**
*
**
***
1
3
6
hours

Figure 3.

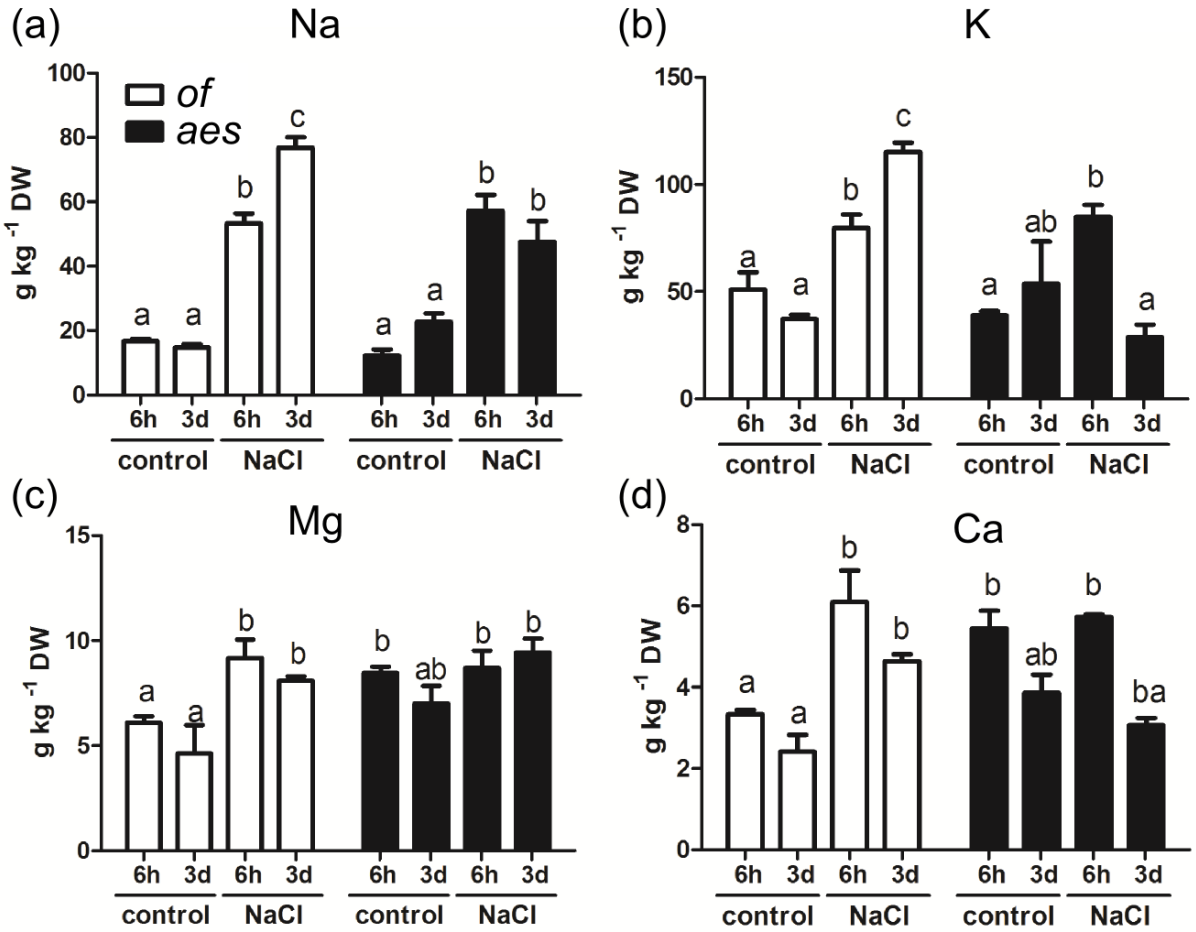

Figure 4.

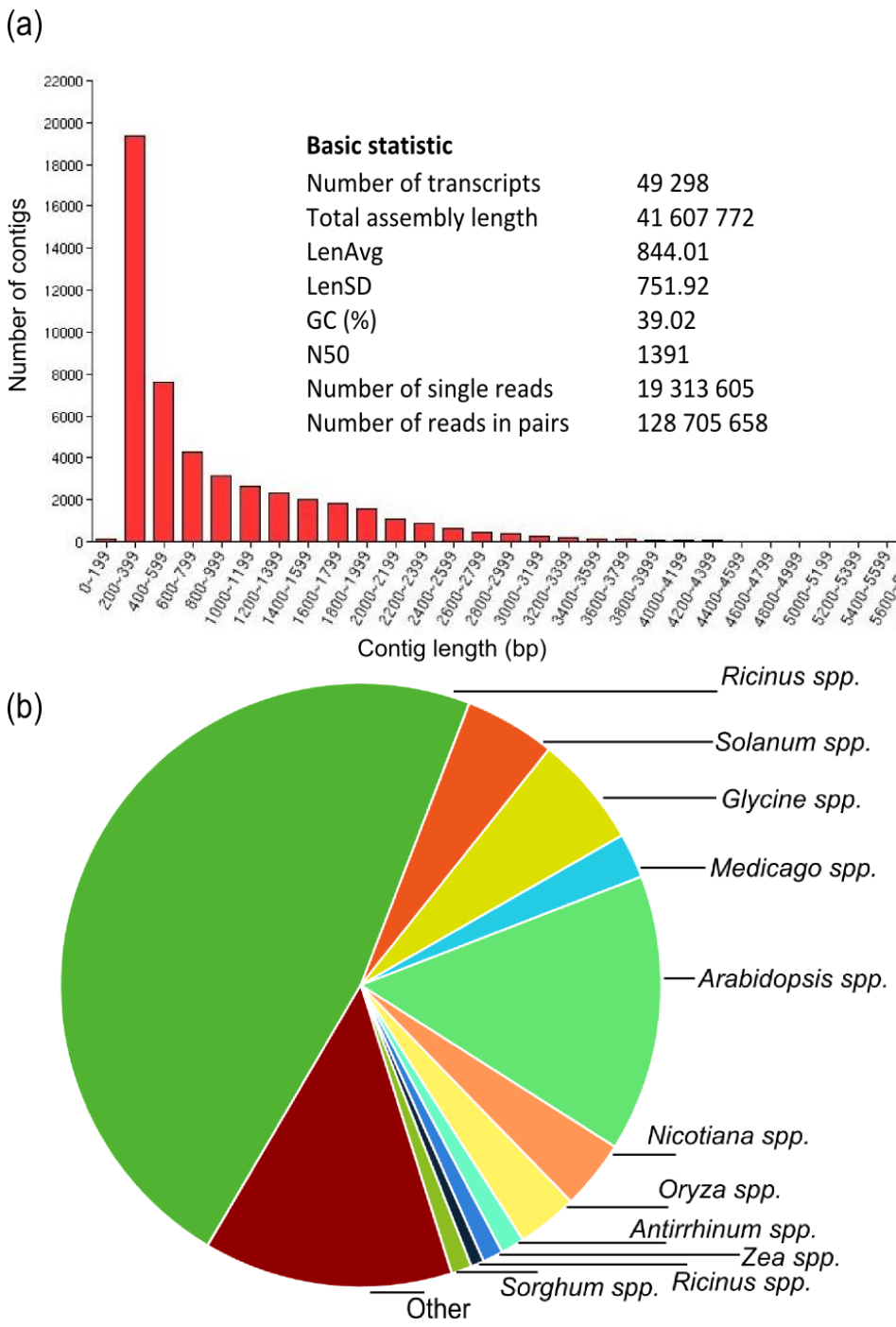
(a)
Number of contigs
Contig length (bp)
Basic statistic
Number of transcripts 49 298
Total assembly length 41 607 772
LenAvg 844.01
LenSD 751.92
GC (%) 39.02
N50 1391
Number of single reads 19 313 605
Number of reads in pairs 128 705 658
(b)
Ricinus spp.
Solanum spp.
Glycine spp.
Medicago spp.
Arabidopsis spp.
Nicotiana spp.
Oryza spp.
Antirrhinum spp.
Zea spp.
Sorghum spp.
Ricinus spp.
Other

Figure 5.

(a)

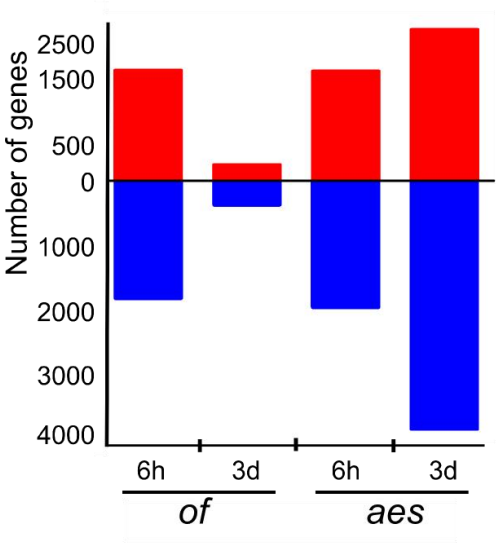

(b)

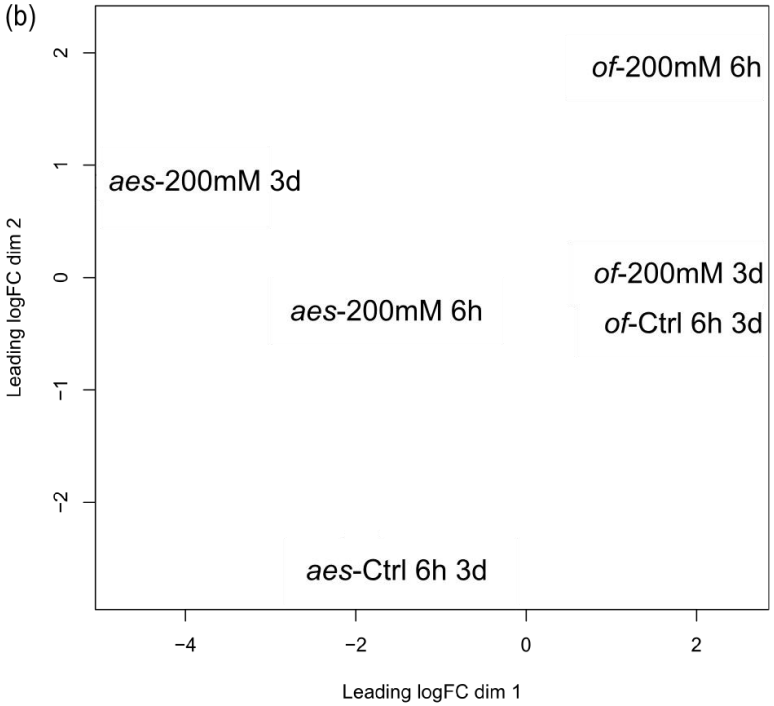

(c)

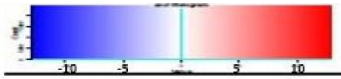

#Term	KEGG ID	Input #	Background #	P-Value	Clusters
cAMP signaling pathway	ko04024	7	8	3.18E-05	1
Carbon fixation in photosynthetic organisms	ko00710	13	25	1.11E-06	4
Cell cycle	ko04110	9	58	0.003069	10, 18
DNA replication	ko03030	9	32	2.19E-05	10
Fatty acid metabolism	ko01212	9	28	0.002696	2
MAPK signaling pathway	ko04010	5	8	0.002885	2
Phenylpropanoid biosynthesis	ko00940	13	23	2.05E-06	5, 14
Photosynthesis	ko00195	18	55	0.000221	4
Photosynthesis antenna proteins	ko00196	8	12	0.000408	4
Plant hormone signaling pathway	ko04075	30	43	1.40E-05	1, 2, 15

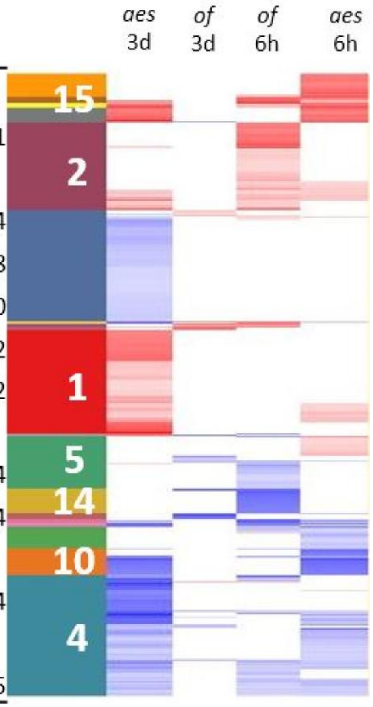

Figure 6.

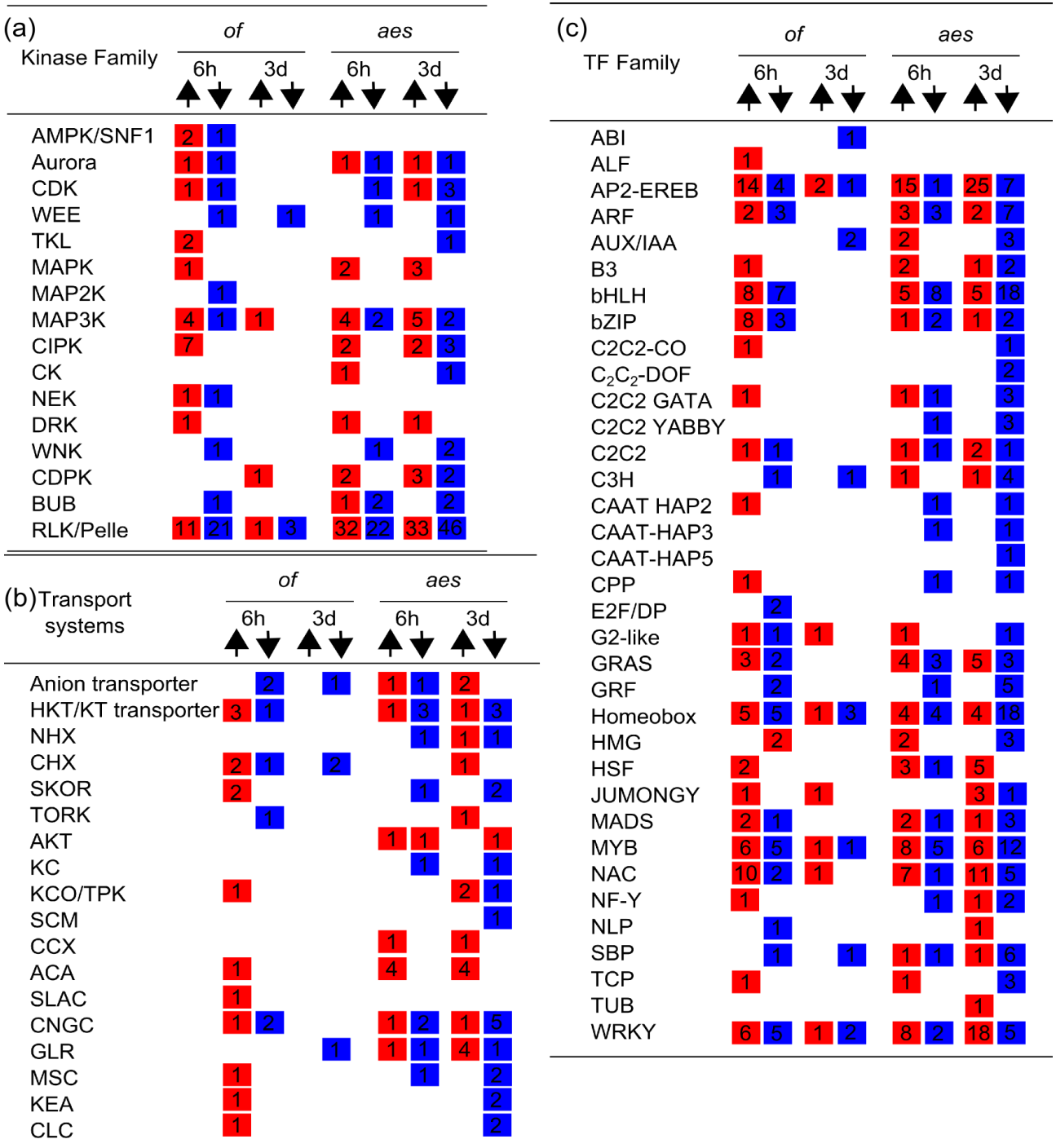
(a)
Kinase Family
of
aes
6h
3d
6h
3d
AMPK/SNF1
Aurora
CDK
WEE
TKL
MAPK
MAP2K
MAP3K
CIPK
CK
NEK
DRK
WNK
CDPK
BUB
RLK/Pelle
(b)Transport systems
of
aes
6h
3d
6h
3d
Anion transporter
HKT/KT transporter
NHX
CHX
SKOR
TORK
AKT
KC
KCO/TPK
SCM
CCX
ACA
SLAC
CNGC
GLR
MSC
KEA
CLC
(c)
TF Family
of
aes
6h
3d
6h
3d
ABI
ALF
AP2-EREB
ARF
AUX/IAA
B3
bHLH
bZIP
C2C2-CO
C2C2-DOF
C2C2 GATA
C2C2 YABBY
C2C2
C3H
CAAT HAP2
CAAT-HAP3
CAAT-HAP5
CPP
E2F/DP
G2-like
GRAS
GRF
Homeobox
HMG
HSF
JUMONGY
MADS
MYB
NAC
NF-Y
NLP
SBP
TCP
TUB
WRKY

Figure 7.

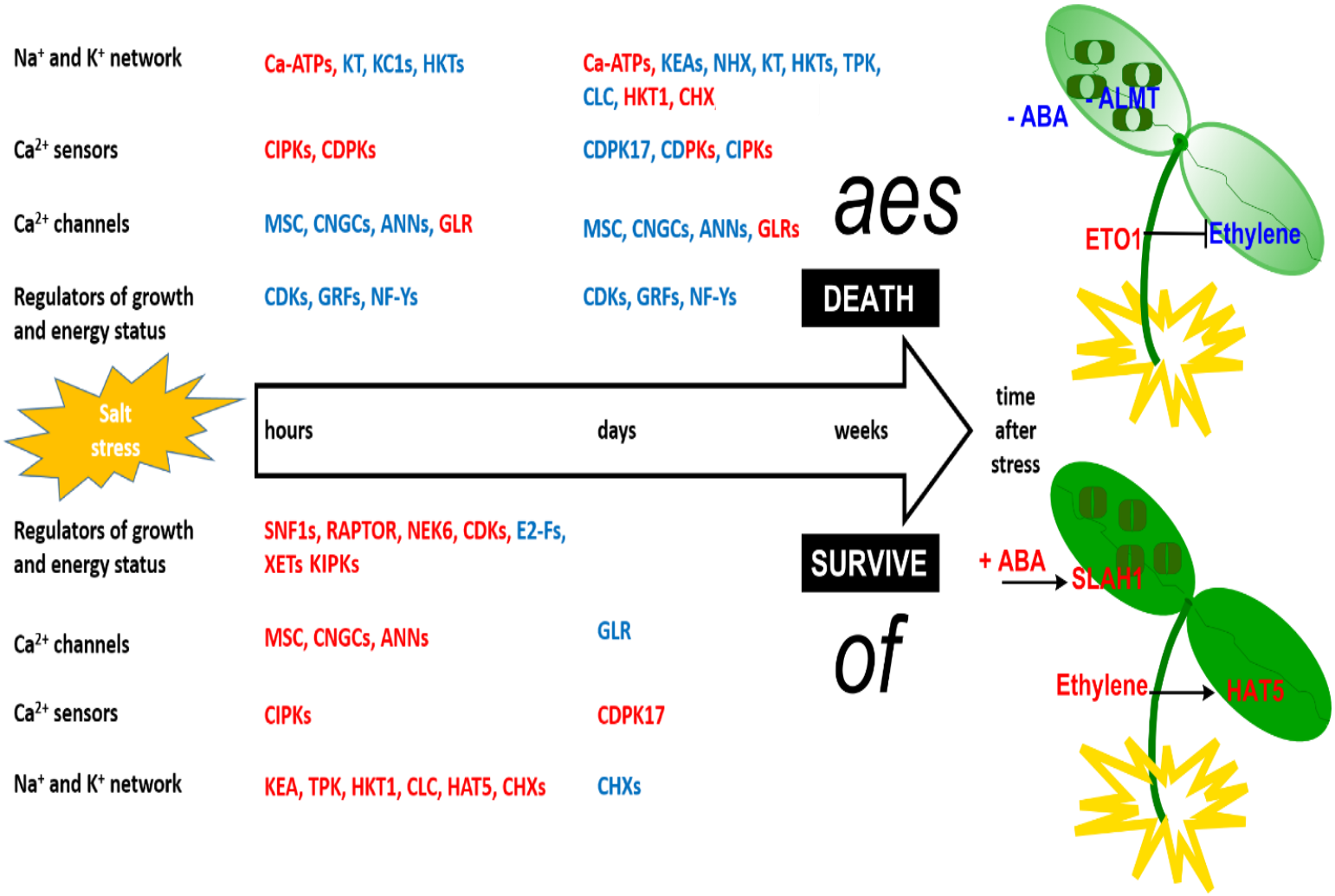
Na+ and K+ network
Ca-ATPs, KT, KC1s, HKTs
Ca-ATPs, KEAs, NHX, KT, HKTs, TPK, CLC, HKT1, CHX
Ca2+ sensors
CIPKs, CDPKs
CDPK17, CDPKs, CIPKs
Ca2+ channels
MSC, CNGCs, ANNs, GLR
MSC, CNGCs, ANNs, GLRs
Regulators of growth and energy status
CDKs, GRFs, NF-Ys
CDKs, GRFs, NF-Ys
aes
DEATH
Salt stress
hours
days
weeks
time after stress
Regulators of growth and energy status
SNF1s, RAPTOR, NEK6, CDKs, E2-Fs, XETs KIPKs
SURVIVE
Ca2+ channels
MSC, CNGCs, ANNs
GLR
of
Ca2+ sensors
CIPKs
CDPK17
Na+ and K+ network
KEA, TPK, HKT1, CLC, HAT5, CHXs
CHXs
- ABA
- ALMT
ETO1
Ethylene
+ ABA
SLAH1
Ethylene
HAT5

Figure S1.

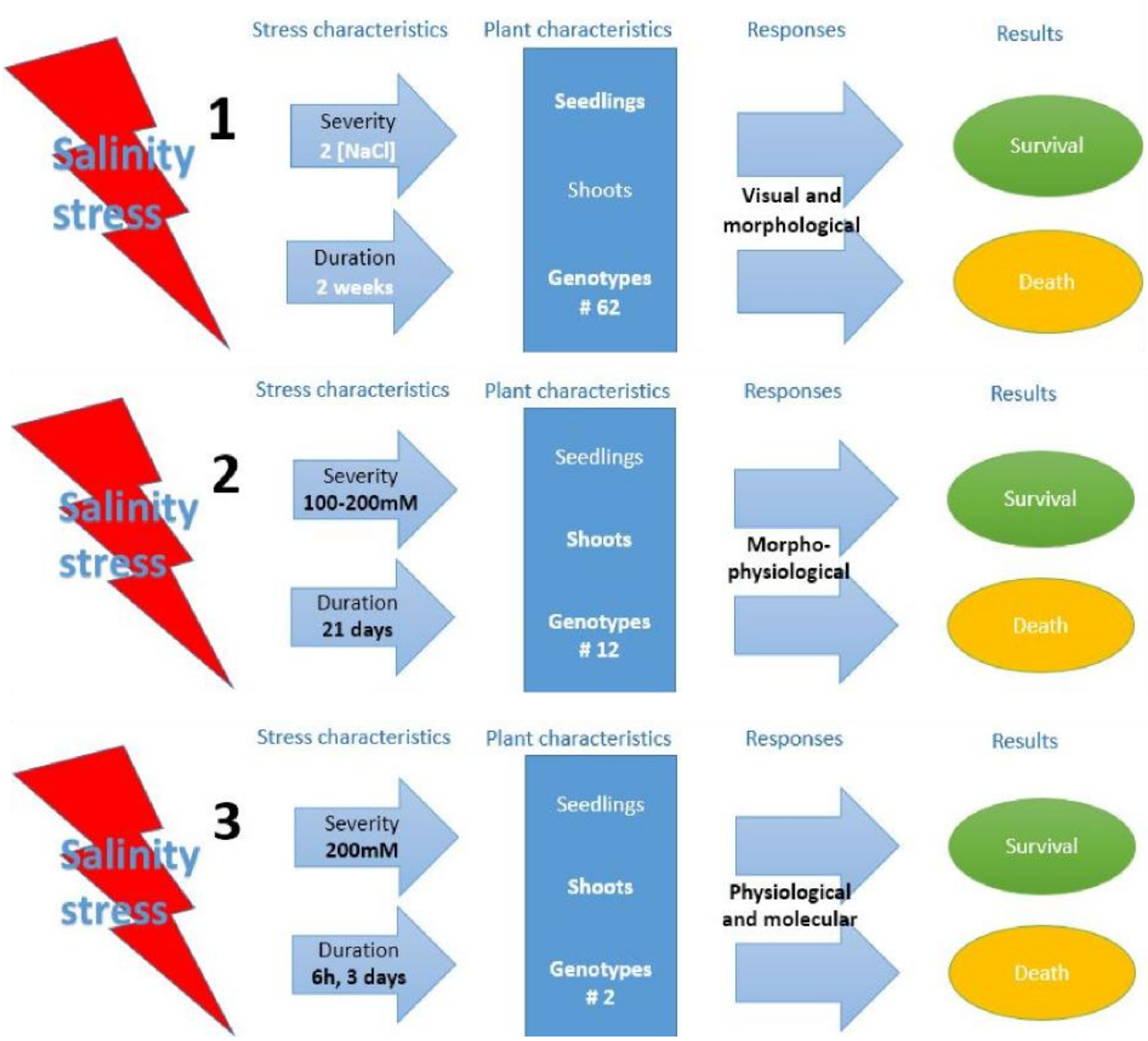
Stress characteristics
Plant characteristics
Responses
Results
1
Salinity stress
Severity 2 [NaCl]
Duration 2 weeks
Seedlings
Shoots
Genotypes # 62
Visual and morphological
Survival
Death
2
Salinity stress
Severity 100-200mM
Duration 21 days
Seedlings
Shoots
Genotypes # 12
Morpho-physiological
Survival
Death
3
Salinity stress
Severity 200mM
Duration 6h, 3 days
Seedlings
Shoots
Genotypes # 2
Physiological and molecular
Survival
Death

Figure S2.

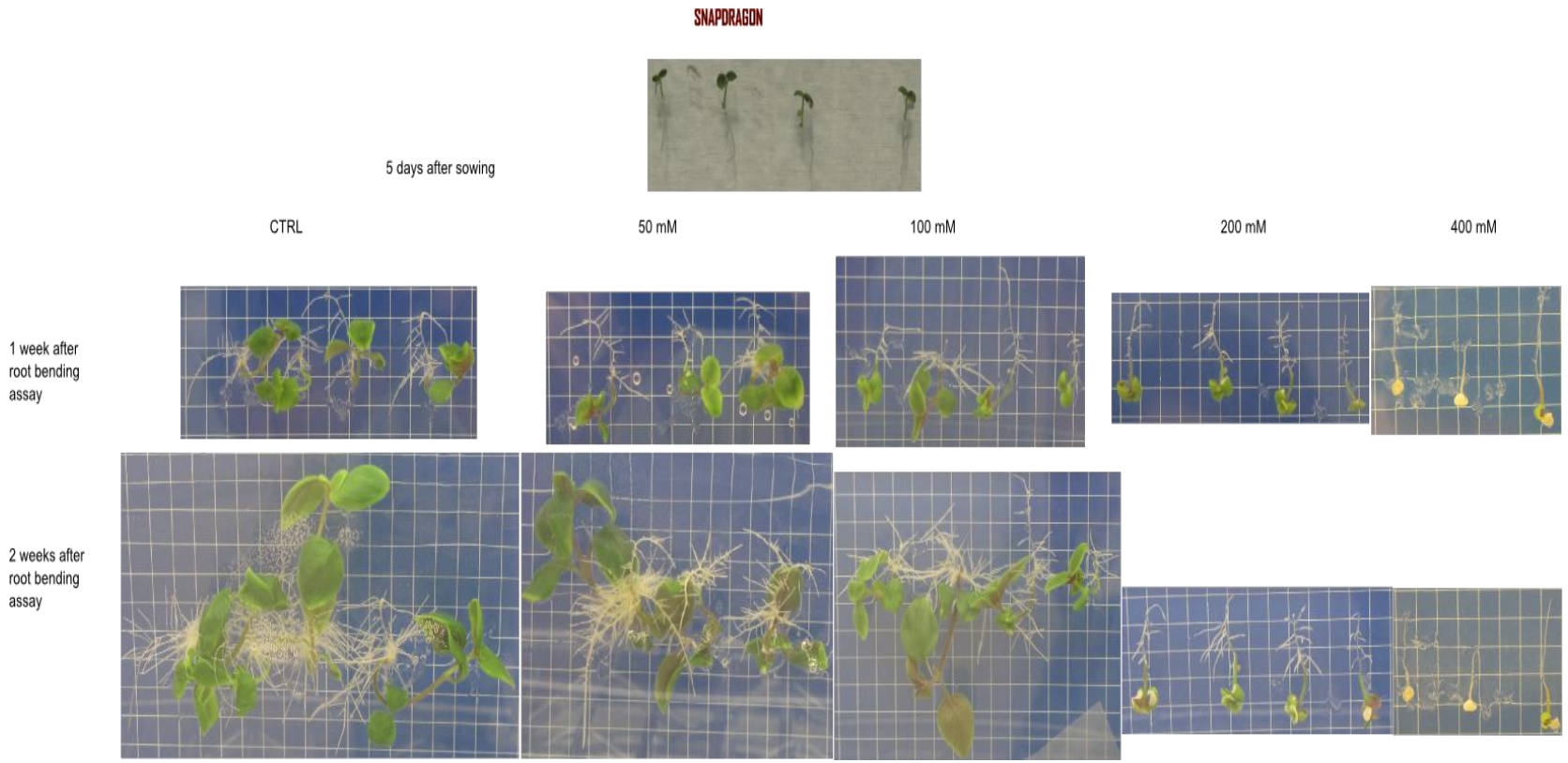
SNAPDRAGON
5 days after sowing
CTRL
50 mM
100 mM
200 mM
400 mM
1 week after root bending assay
2 weeks after root bending assay

Figure S3.

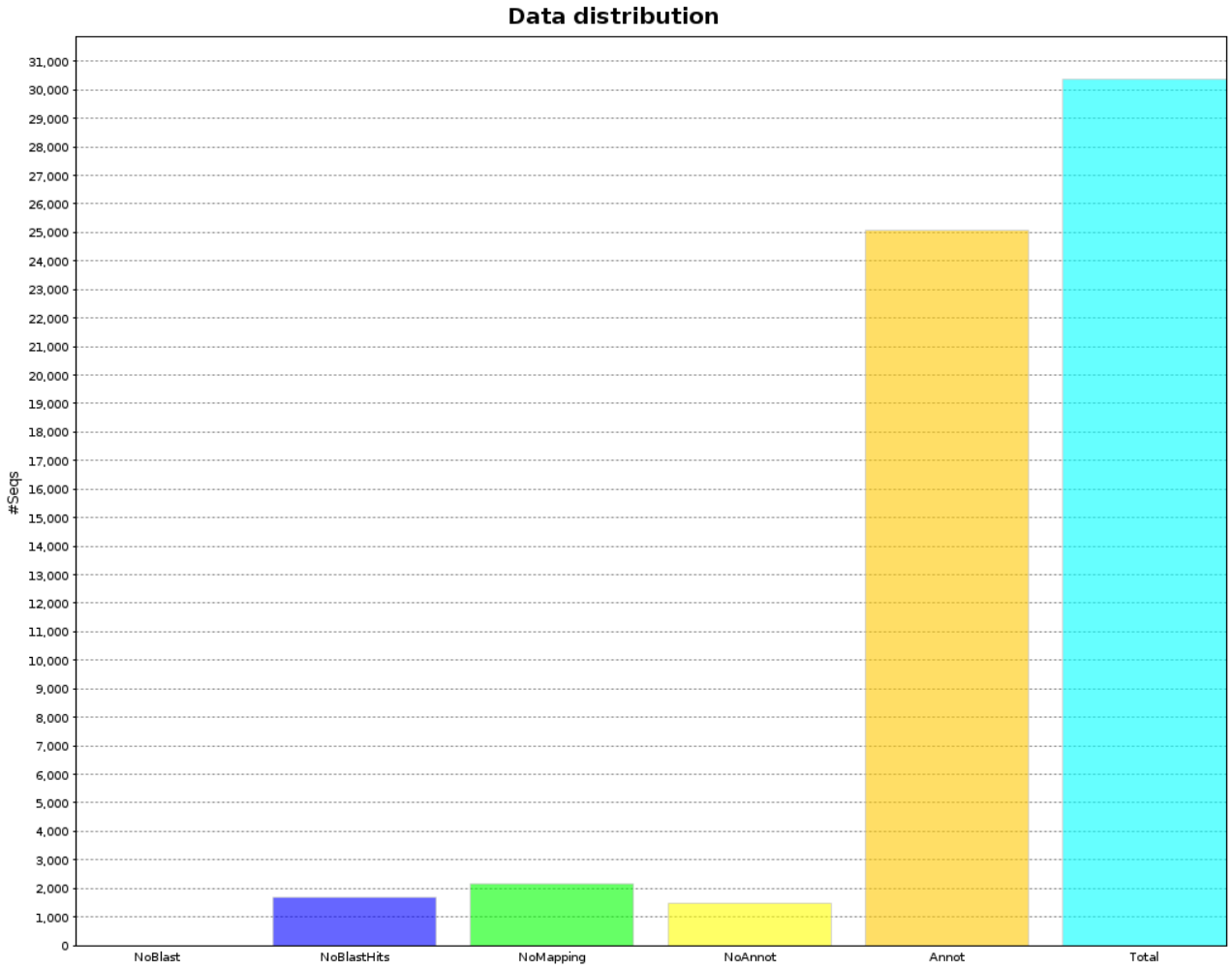
Data distribution
#Seqs
31,000
30,000
29,000
28,000
27,000
26,000
25,000
24,000
23,000
22,000
21,000
20,000
19,000
18,000
17,000
16,000
15,000
14,000
13,000
12,000
11,000
10,000
9,000
8,000
7,000
6,000
5,000
4,000
3,000
2,000
1,000
0
NoBlast
NoBlastHits
NoMapping
NoAnnot
Annot
Total

Figure S4.

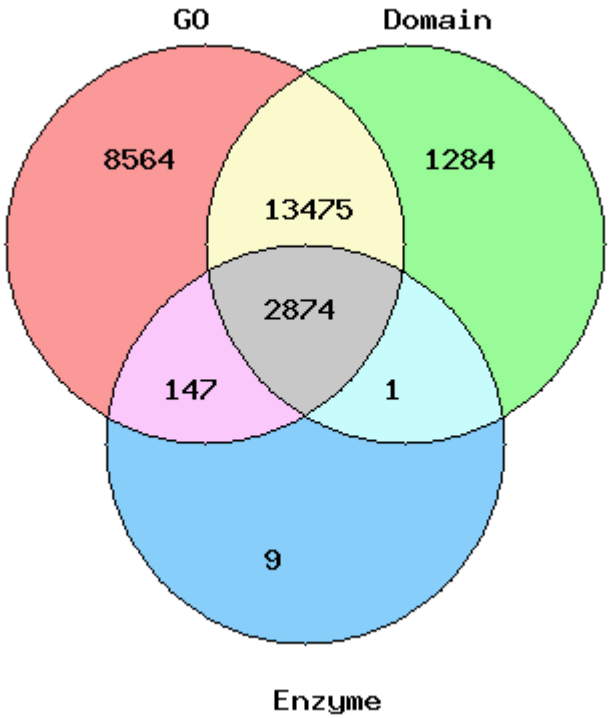

Figure S5

45 (a)

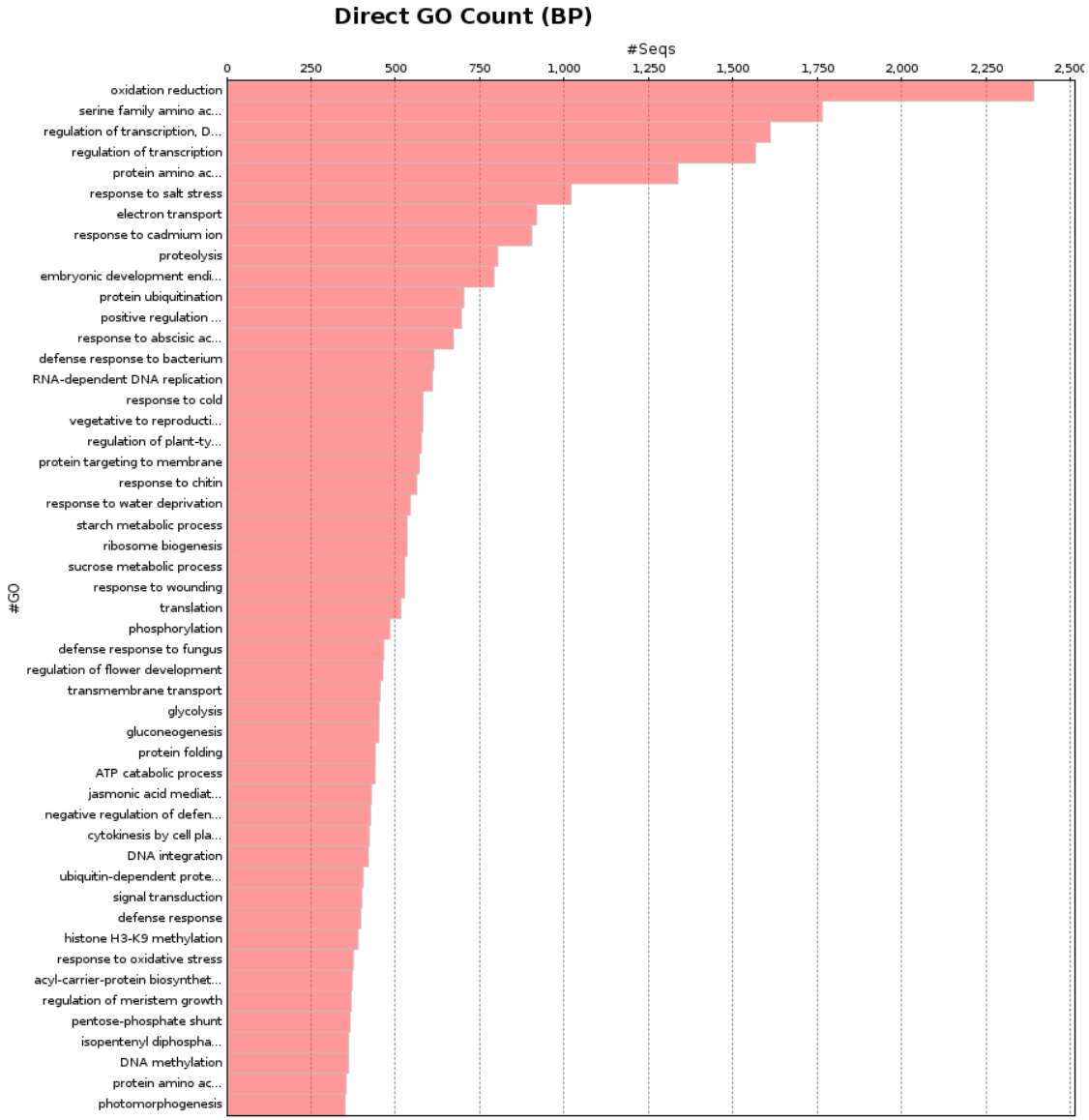
Direct GO Count (BP)
#Seqs
0
250
500
750
1,000
1,250
1,500
1,750
2,000
2,250
#GO
oxidation reduction
serine family amino ac...
regulation of transcription, D...
regulation of transcription
protein amino ac...
response to salt stress
electron transport
response to cadmium ion
proteolysis
embryonic development endi...
protein ubiquitination
positive regulation ...
response to abscisic ac...
defense response to bacterium
RNA-dependent DNA replication
response to cold
vegetative to reproducti...
regulation of plant-ty...
protein targeting to membrane
response to chitin
response to water deprivation
starch metabolic process
ribosome biogenesis
sucrose metabolic process
response to wounding
translation
phosphorylation
defense response to fungus
regulation of flower development
transmembrane transport
glycolysis
gluconeogenesis
protein folding
ATP catabolic process
jasmonic acid mediat...
negative regulation of defen...
cytokinesis by cell pla...
DNA integration
ubiquitin-dependent prote...
signal transduction
defense response
histone H3-K9 methylation
response to oxidative stress
acyl-carrier-protein biosynthet...
regulation of meristem growth
pentose-phosphate shunt
isopentenyl diphospha...
DNA methylation
protein amino ac...
photomorphogenesis

46

47 (b)

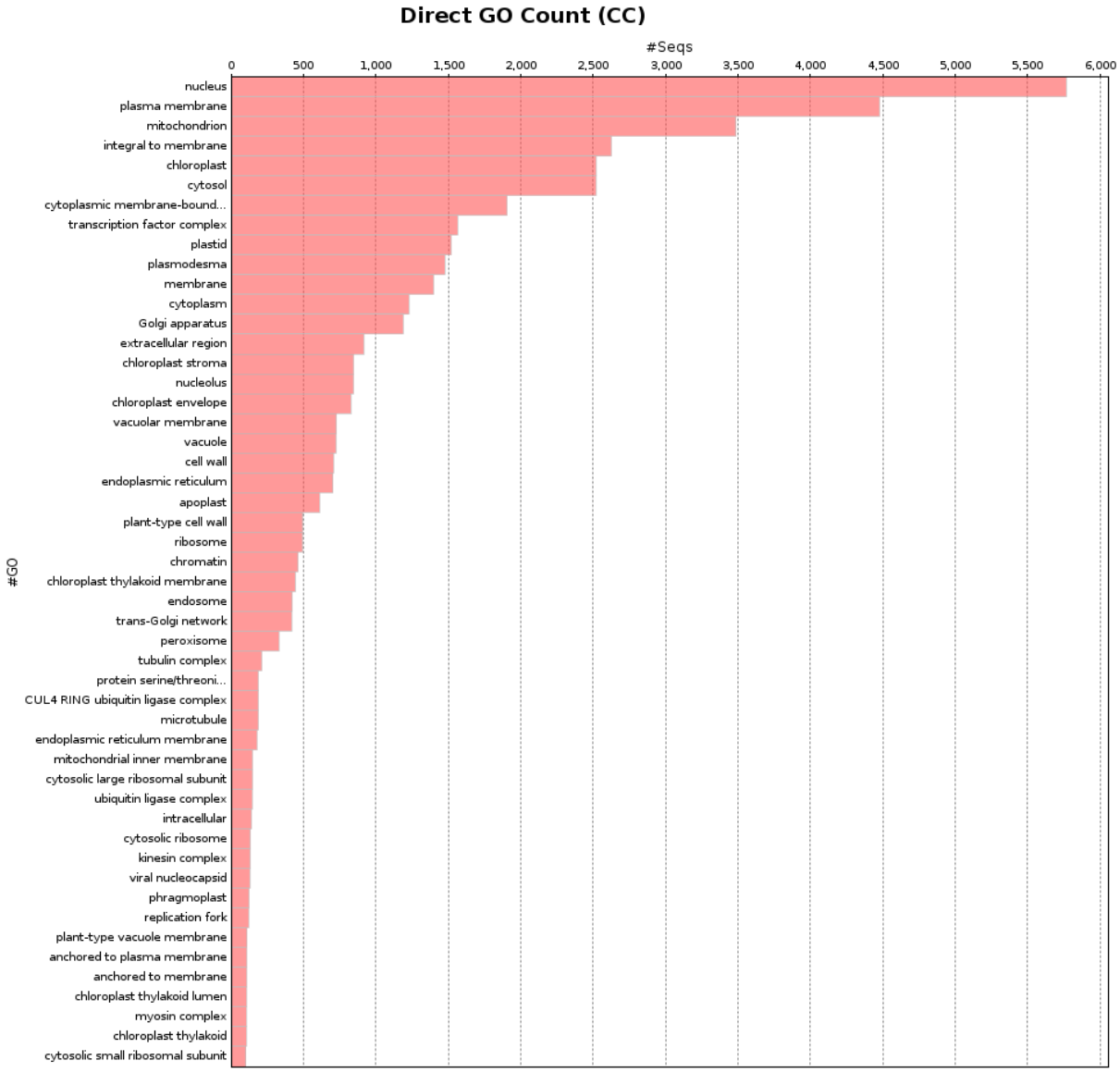
Direct GO Count (CC)
#Seqs
0
500
1,000
1,500
2,000
2,500
3,000
3,500
4,000
4,500
5,000
5,500
6,000
#GO
nucleus
plasma membrane
mitochondrion
integral to membrane
chloroplast
cytosol
cytoplasmic membrane-bound...
transcription factor complex
plastid
plasmodesma
membrane
cytoplasm
Golgi apparatus
extracellular region
chloroplast stroma
nucleolus
chloroplast envelope
vacuolar membrane
vacuole
cell wall
endoplasmic reticulum
apoplast
plant-type cell wall
ribosome
chromatin
chloroplast thylakoid membrane
endosome
trans-Golgi network
peroxisome
tubulin complex
protein serine/threoni...
CUL4 RING ubiquitin ligase complex
microtubule
endoplasmic reticulum membrane
mitochondrial inner membrane
cytosolic large ribosomal subunit
ubiquitin ligase complex
intracellular
cytosolic ribosome
kinesin complex
viral nucleocapsid
phragmoplast
replication fork
plant-type vacuole membrane
anchored to plasma membrane
anchored to membrane
chloroplast thylakoid lumen
myosin complex
chloroplast thylakoid
cytosolic small ribosomal subunit

48

(c)

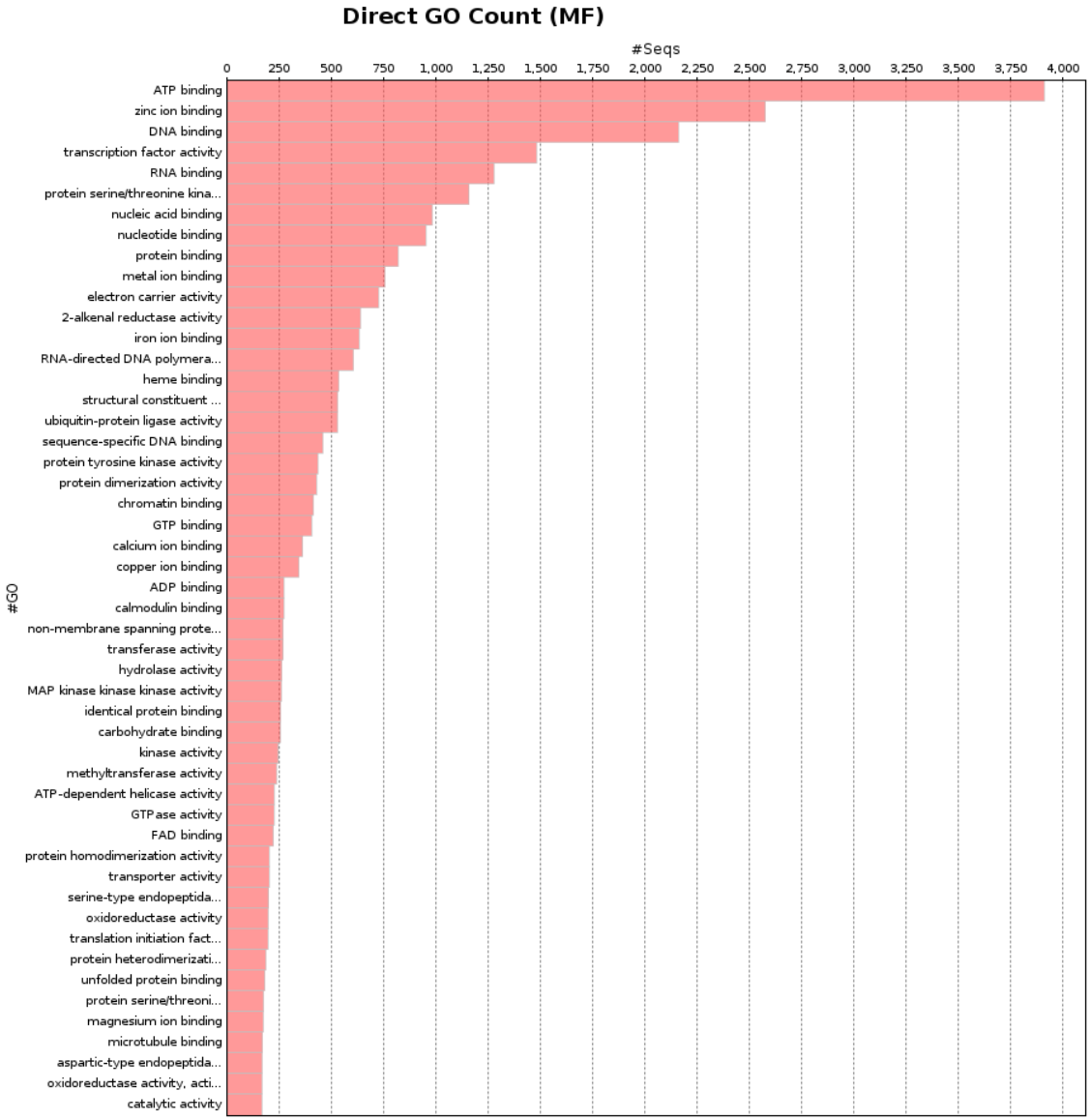
Direct GO Count (MF)
#Seqs
0
250
500
750
1,000
1,250
1,500
1,750
2,000
2,250
2,500
2,750
3,000
3,250
3,500
3,750
4,000
#GO
ATP binding
zinc ion binding
DNA binding
transcription factor activity
RNA binding
protein serine/threonine kina...
nucleic acid binding
nucleotide binding
protein binding
metal ion binding
electron carrier activity
2-alkenal reductase activity
iron ion binding
RNA-directed DNA polymera...
heme binding
structural constituent ...
ubiquitin-protein ligase activity
sequence-specific DNA binding
protein tyrosine kinase activity
protein dimerization activity
chromatin binding
GTP binding
calcium ion binding
copper ion binding
ADP binding
calmodulin binding
non-membrane spanning prote...
transferase activity
hydrolase activity
MAP kinase kinase kinase activity
identical protein binding
carbohydrate binding
kinase activity
methyltransferase activity
ATP-dependent helicase activity
GTPase activity
FAD binding
protein homodimerization activity
transporter activity
serine-type endopeptida...
oxidoreductase activity
translation initiation fact...
protein heterodimerizati...
unfolded protein binding
protein serine/threoni...
magnesium ion binding
microtubule binding
aspartic-type endopeptida...
oxidoreductase activity, acti...
catalytic activity

Figure S6.

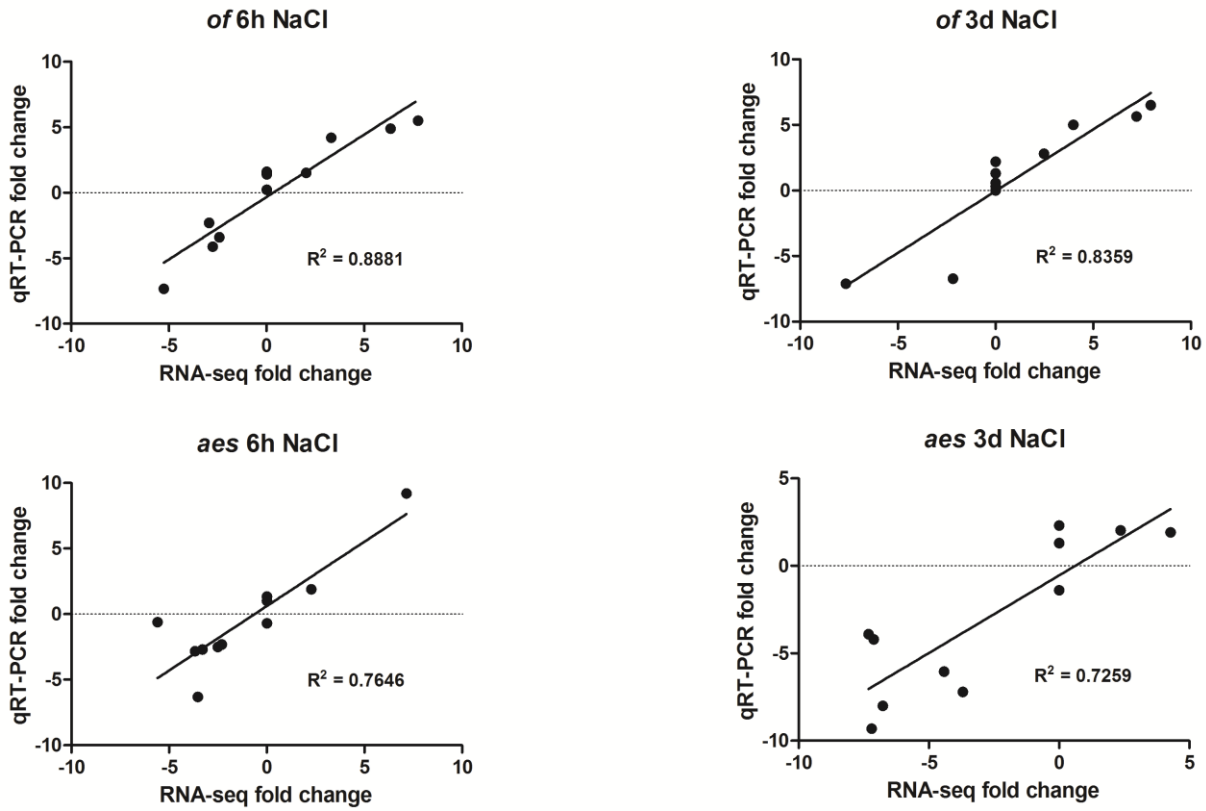
of 6h NaCl
qRT-PCR fold change
RNA-seq fold change
R^2 = 0.8881
of 3d NaCl
R^2 = 0.8359
aes 6h NaCl
R^2 = 0.7646
aes 3d NaCl
R^2 = 0.7259

Figure S7.

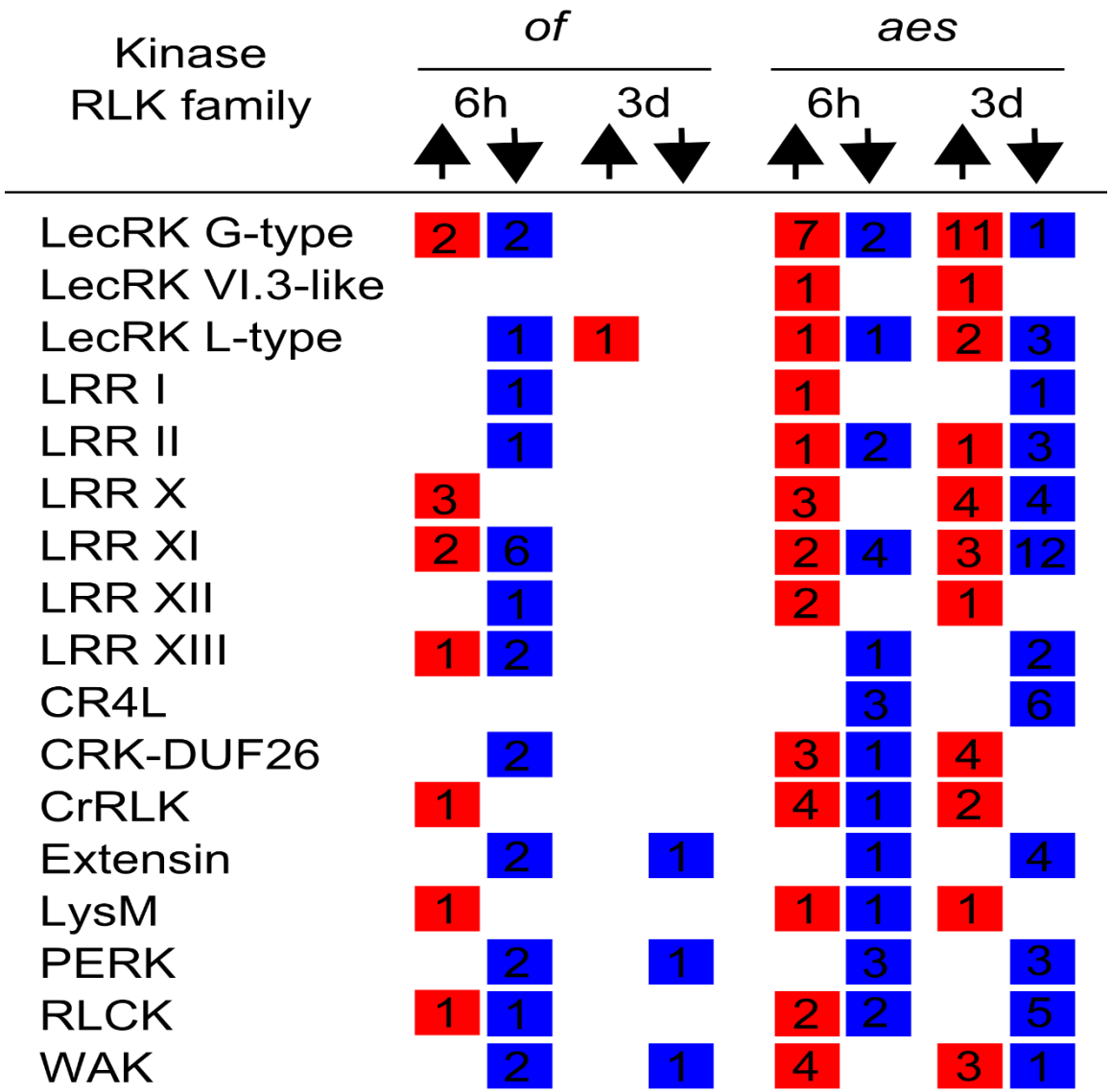
Kinase
RLK family
of
aes
6h
3d
6h
3d
LecRK G-type 2 2 7 2 11 1
LecRK VI.3-like 1 1
LecRK L-type 1 1 1 1 2 3
LRR I 1 1 1
LRR II 1 1 2 1 3
LRR X 3 3 4 4
LRR XI 2 6 2 4 3 12
LRR XII 1 2 1
LRR XIII 1 2 1 2
CR4L 3 6
CRK-DUF26 2 3 1 4
CrRLK 1 4 1 2
Extensin 2 1 1 4
LysM 1 1 1 1
PERK 2 1 3 3
RLCK 1 1 2 2 5
WAK 2 1 4 3 1

Figure S8.

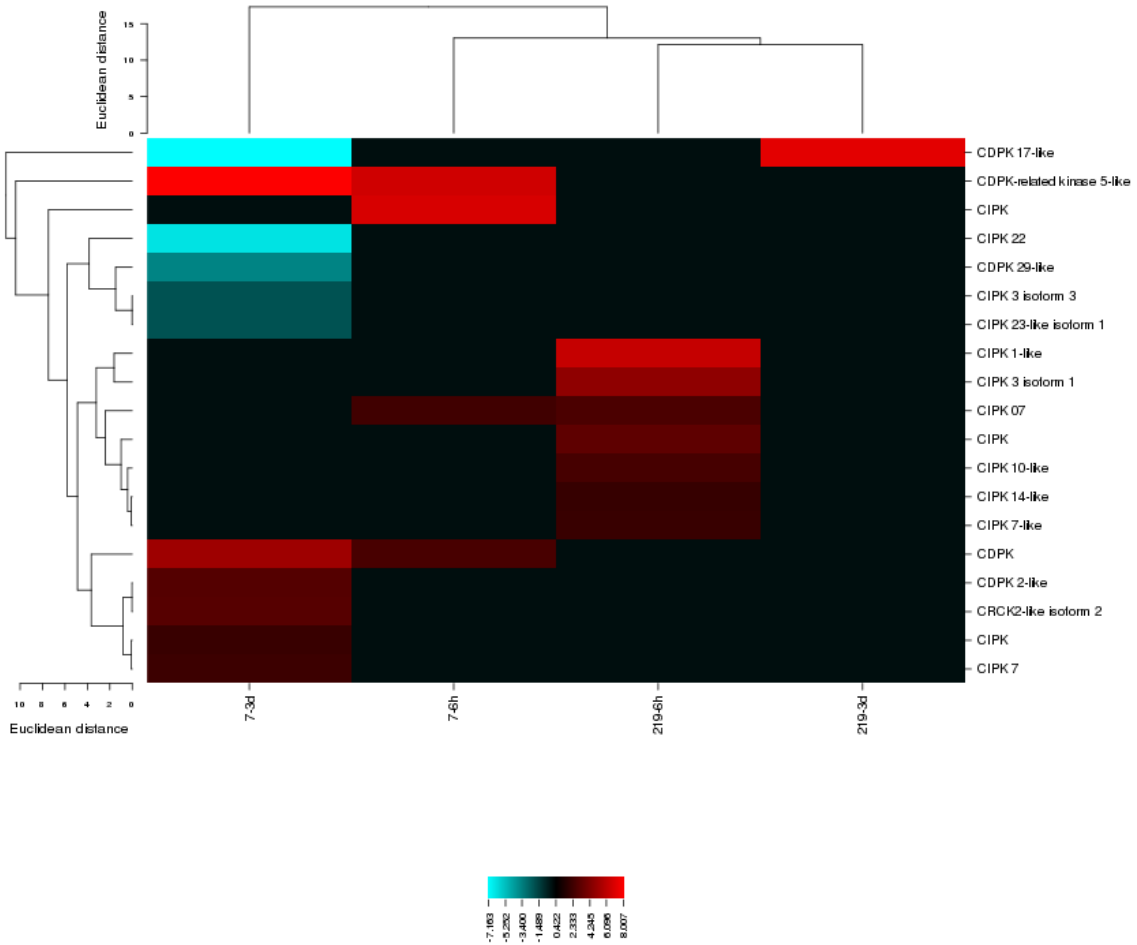
Euclidean distance
CDPK 17-like
CDPK-related kinase 5-like
CIPK
CIPK 22
CDPK 29-like
CIPK 3 isoform 3
CIPK 23-like isoform 1
CIPK 1-like
CIPK 3 isoform 1
CIPK 07
CIPK
CIPK 10-like
CIPK 14-like
CIPK 7-like
CDPK
CDPK 2-like
CRCK2-like isoform 2
CIPK
CIPK 7
7-3d
7-6h
219-6h
219-3d
Euclidean distance

Figure S9

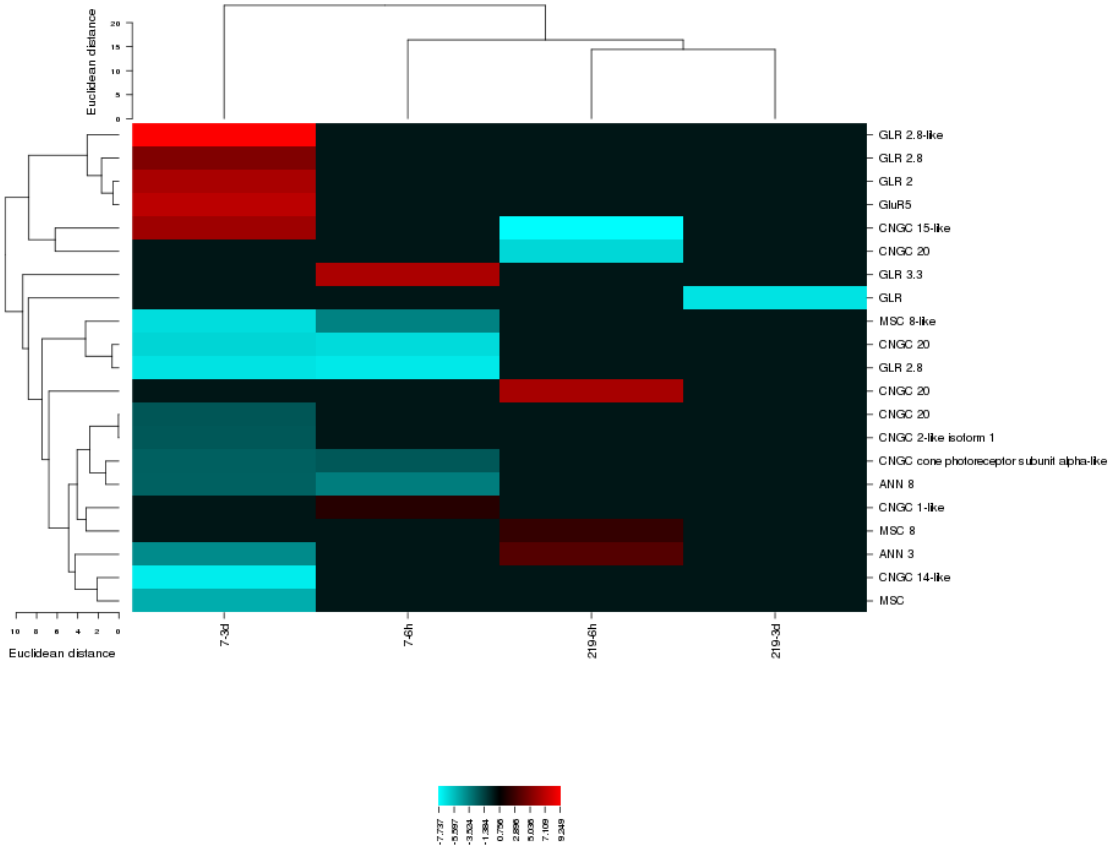
Euclidean distance
GLR 2.8-like
GLR 2.8
GLR 2
GluR5
CNGC 15-like
CNGC 20
GLR 3.3
GLR
MSC 8-like
CNGC 20
GLR 2.8
CNGC 20
CNGC 20
CNGC 2-like isoform 1
CNGC cone photoreceptor subunit alpha-like
ANN 8
CNGC 1-like
MSC 8
ANN 3
CNGC 14-like
MSC
7-3d
7-6h
219-6h
219-3d
Euclidean distance

72 **Figure S10**

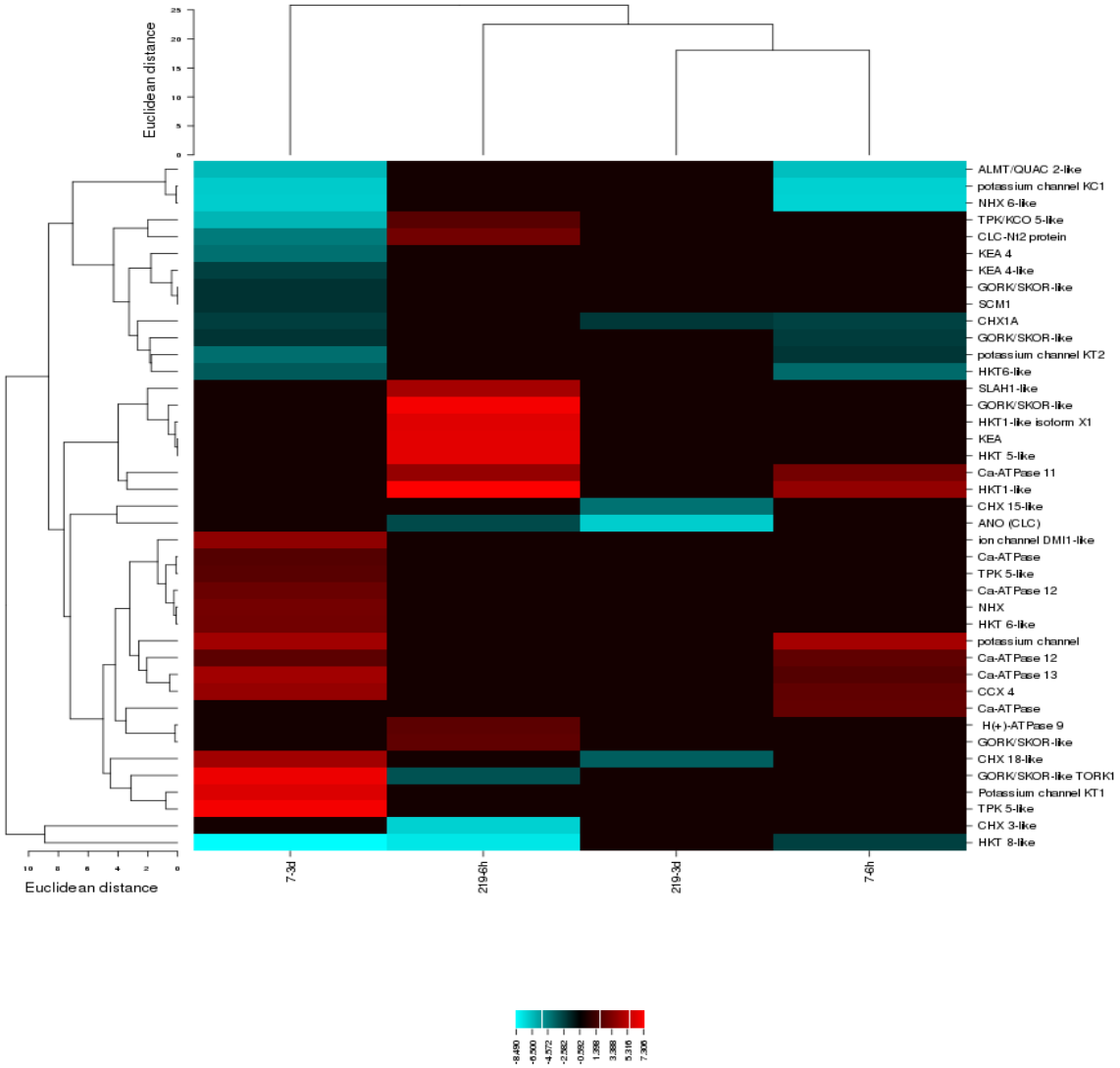

73

74

Figure S11

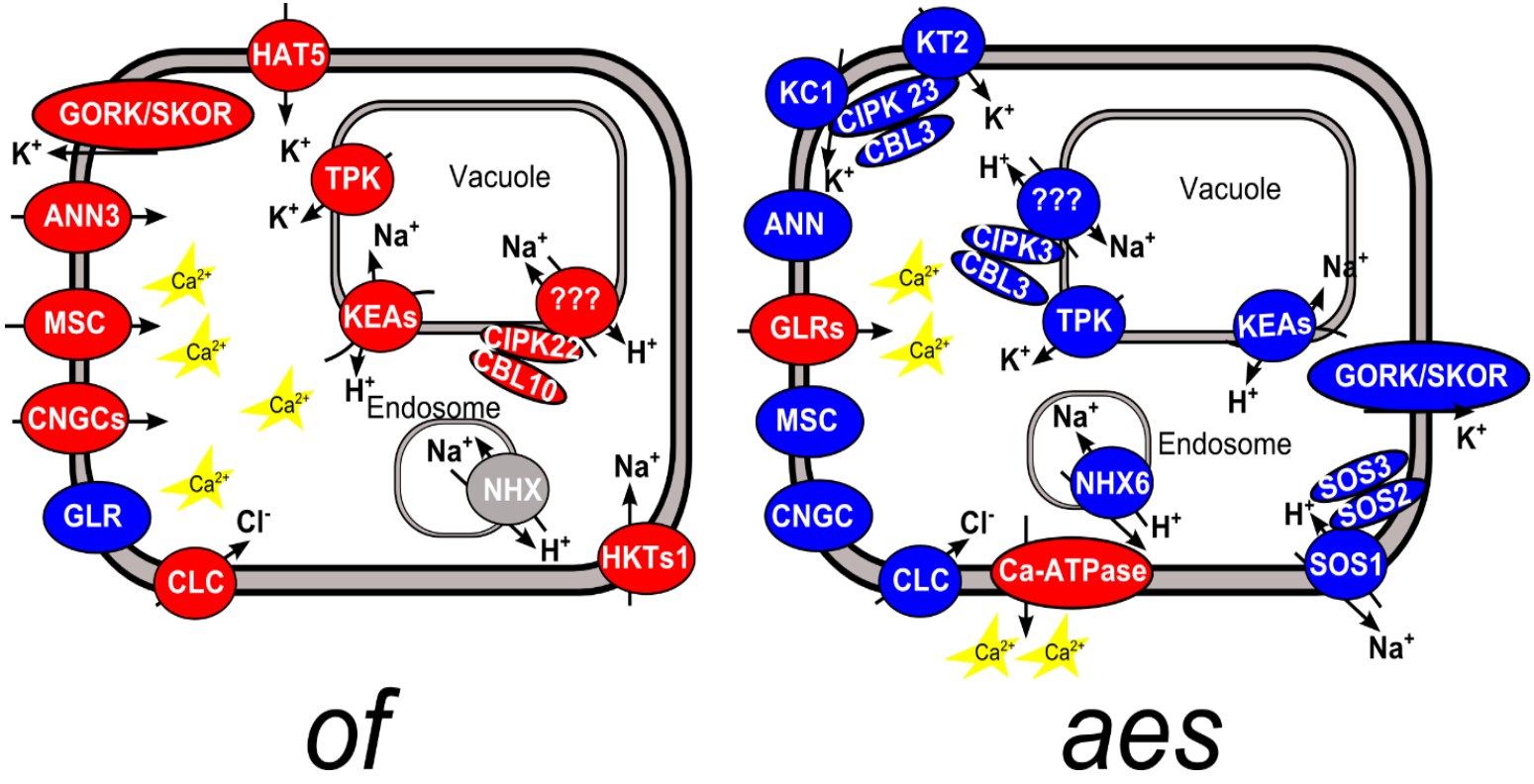
HAT5
GORK/SKOR
K+
ANN3
MSC
CNGCs
GLR
CLC
Cl-
Ca2+
TPK
Vacuole
KEAs
???
CIPK22
CBL10
H+
Endosome
Na+
NHX
HKTs1
of
KT2
KC1
CIPK 23
CBL3
ANN
GLRs
MSC
CNGC
CLC
CIPK3
TPK
KEAs
GORK/SKOR
NHX6
SOS3
SOS2
SOS1
Ca-ATPase
aes

84 **Figure S12**

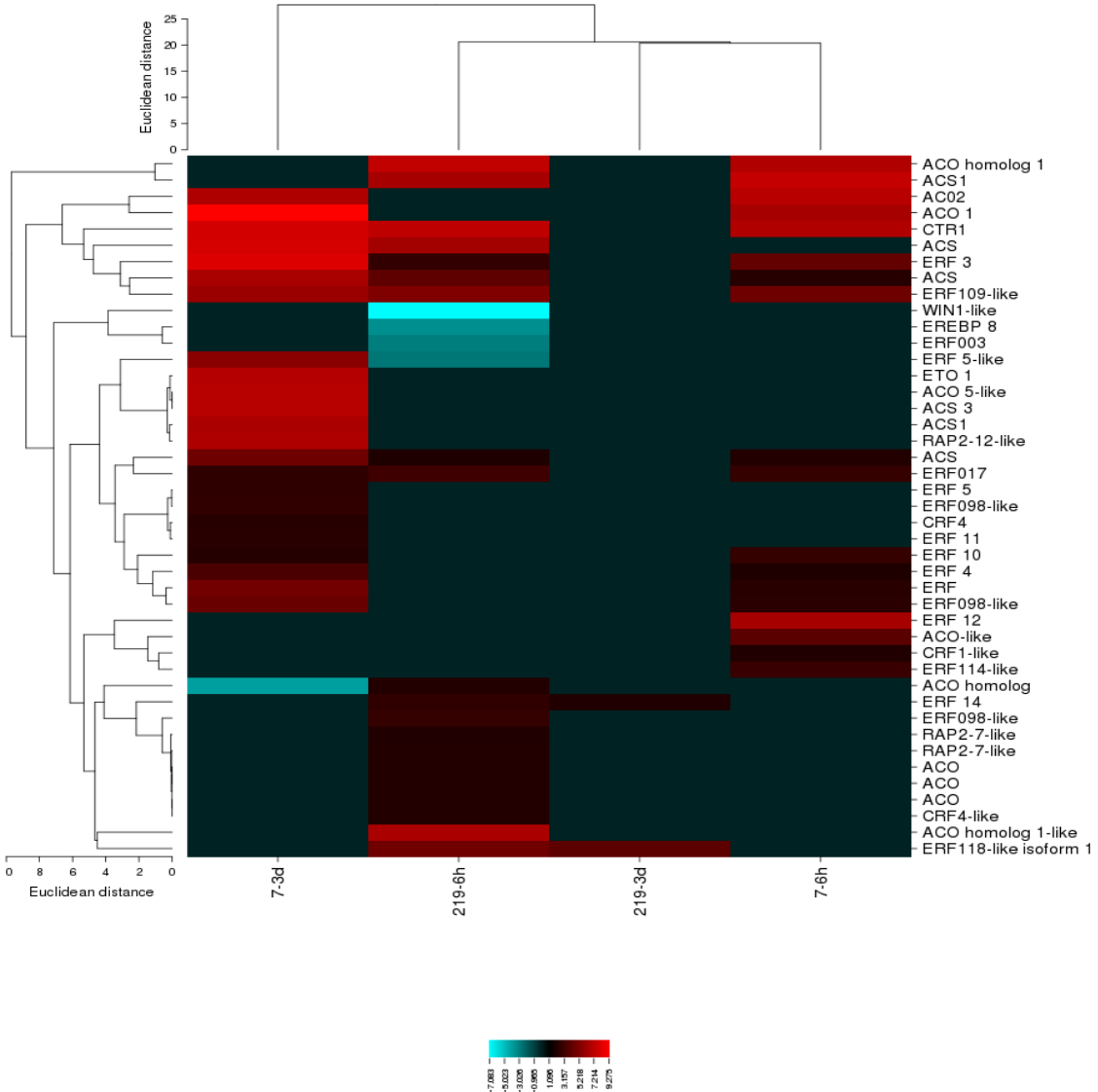

85

Supplementary tables

Table S1 List of *Antirrhinum majus* mutants screened using using a root-bending assay at 100 and 300 mM NaCl. The 62 mutants were selected among more than 450 genotypes for their phenotype description provided by the snapdragon database, DragonDB (http://www.antirrhinum.net/). Seeds were surface sterilized by soaking in a solution of sodium hypochlorite 20% plus 0.01% Triton X-I00 for 10 min and rinsing four times with sterile water. The seeds were plated on MS agar medium (Murashige and Skoog, 1962) with 3% (w/v) sucrose and 4% (w/v) Gelrite®, pH 5.7. The plates were stored at 4°C for 48 hr to improve germination uniformity.

The phenotype under salt stress were visually assessed. A seedling was considered green when both cotyledons and stem tissues appeared to be totally green as the control (XXX). A seedling was considered de-greening/yellowish (XX) when at least 50% of the tissues-color was degraded. A seedling was considered bleached (X) when the entire tissue was white.

Locus name	MAM ids	Mutant name*	Gene*	*Phenotype description	Visual bleaching/degreening			
					100mM NaCl		300mM NaCl	
					1 week	2 week	1 week	2 week
AC	2	ACCUMBENS	ac	The plantlets are slightly bend in the beginning. Their main axis bends later on und the side shoots grow tortuously. Grown plants lie flat on the ground. Leaves are somewhat smaller and narrower than normal. In grown up plants the lower leaves are broad, thick, of a darker green color. The upper leaves are small, short, narrow and pointed.	xxx	xxx	xx	xx

AEG	5	AEGROTA	aeg	Habit: Grown plants strong and healthy with stiff growth. Leaves: Seedlings often show cup shaped leaflets. Later leaves rounded, broader than normal. Leaves have a blue-green color with almost parallel veins. Seedlings: 'Sick' appearance. Growth strongly retarded. Changes do not affect all seedlings similarly. Seems strongly dependent upon the environment. After a few weeks the growth retardation is overcome by most of the seedlings.	xxx	xxx	xx	xx
AES	7	AESTIVA	aes	Habit: Growth retarded. Bushy plants. Leaves: Dark green, shiny. Smaller and more pointed than normal. Somewhat wavy, edges bend upwards.	xxx	xxx	x	x
ARB	23	ARBUSCULA	arb	Habit: Small plants, short side shoots, slender growth. Leaves: light green to olive green. Somewhat smaller and undulated.	xxx	xxx	xx	xx
ARR	25	ARRECTA	arr	Habit: Flowering plants with almost normal growth. Leaves: Smaller and upwards bended. Flowering plants with dark green, long and narrow leaves. Cotyledons somewhat lighter and rounder than in Sippe 50. First pair of normal leaves develops late.	xxx	xxx	xx	x
BAD	29	BADIIFOLIA	bad	Habit: Plants are small and narrow. Leaves are small and have a red brown color (due to much anthocyanin). The leaves are bend upwards like a spoon. In older plants almost all leaves are show the mutant trait.	xxx	xxx	xx	xx
COA	55	COARCTATA	coa	Habit: Plants small and dwarfed. Bushy growth. Many small leaves. Seedlings: Hypocotyl short.	xxx	xxx	xx	xx
CONS	62	CONSPERSA	cons	Leaves: In Young plants leaves with irregular white patches. Leaves have irregular forms, are bent and twisted. Leaves with much anthocyanin. Cotyledons: whitish green with green edge.	purple	purple	purple	purple
CORF	64	CORRIEFOLIA	corf	Growth retarded. Leaves dark green. And somewhat shiny. They are stiff and somewhat smaller than normal. Leaves are densely inserted. Cotyledone s greyish green, bulged.	xxx	xxx	xx	xx
CRA	67	CRASSOPHYLLA	cra	Habit: Growth retared, bushy. Leaves narrow, dark green and thickened. Dull shiny. Cotyledons: Short and dark green cotyledons.	xxx	xxx	xx	x

DES	85	DECRESCENS	des	Habit: Plats with retarded growth and bushy. Long, thin and loose side branches with many leaves. Lighter green. Seed: reduced germination Roots: reduced growth or absent	xxx	xxx	xx	xx
DEPA	93	DEPAUPERATA	depa	Habit: Seedlings smaller than normal, darker green than normal. Young plants strongly retarded. Leaves: Small, borders bend upwards, wavy. Older leaves red colored on borders. Leaf tips necrotic. Cotyledons: Obliquely bend upwards.	xxx	xxx	xx	x
ERY	119	ERYTRYTHRINA	ery	Young plants dark green leaves. Leaves are bent upwards and with much red color	xxx	xxx	xx	xx
FUL	140	FULVA	ful	Habit: Normal. Side shoots are somewhat longer than normal. The color of the leaves is yellow green. The colour of the cotyledones is yellow green.	xxx	xxx	xx	xx
GLOB	144	GLOBULARIS	glob	Habit: Young plants are small. Plants in the field are uniformly short and bushy. Leaves are short. The color of the leaves has more red than normal. Lower leaves are rounded and rolled inwardly.	xxx	xxx	xx	xx
GRAM	147	GRAMINIFOLIA	gram-mut		xxx	xxx	xxx	xx
HERO	151	HEROINA	hero	Habit: Young plants are stronger than normal. Longer than plants of Sippe 50. Lower leaves smaller, rounder and of a darker green than normal.	xxx	xxx	xx	xx
HU	154	HUMILIS	hu	Habit: About a third shorter than wild type. Plants bushy. Young's leaves whitish green but become greener starting from the middle vein. Older leaves are lighter green. Cotyledons are smaller with a whitish green color. Centrally they darker coloured.	xxx	xxx	xx	x
HY	155	HYACINTHA	hy	Habit: Strong but shorter plants. Leaves are broad. Edges often bend upwards. Cotyledone s are small.	xxx	xxx	xx	x
INA	173	INVOLUTA INACAPS	ina	Habit: Plants are of a lighter green color. Leaves are slightly wavy and their edges are bend upwards	xxx	xxx	xx	xx
IR	174	IRREGULARIS	ir	Habit: Plants are strong and shorter than normal. Main stem is thickened. Leaves are somewhat lighter green and broader than normal.	xxx	xxx	xxx	xx

LAN	177	LANGUIDA	lan	Habit: Seedlings have a yellow green color. Plants are smaller than normal. The color is yellowish green. The tips of the shoots show a still lighter color.	xxx	xxx	xx	xx
LAF	181	LATIFRUCTICOSA	laf	Habit: Very small and bread bushes. Color is dark green. Seedlings dwarfed.	xxx	xxx	x	x
LUX	192	LUXURIANS	lux	Short, strong and broad bushes. Height somewhat less than normal. Leaves are big, full green and somewhat shiny. Show vigorous growth.	xxx	xxx	xx	xx
MACI	194	MACILENTA	maci	First pair of leaves stands upright. Leaves are long and very narrow. Middle vein is lighter than normal.	xxx	xxx	xx	xx
MIA	202	MICANTIFOLIA	mia	Habit: Growth is much retarded. Leaves of young plants are light olive green. Later dark green and shiny. Leaves are more narrow than normal and bend upwards at the edges.	xxx	xxx	xx	xx
NA	207	NANA NANA	na-na	**Nana**. Habit: Growth is much retarded. Plants are strong and healthy. Leaves are bend downwards in the beginning, are shorter, broader and lighter than normal. Plants attain a size of 15 to 20 cm. Many side shoots directly below inflorescence.	xxx	xxx	xx	xx
NEA	210	NERVATIFOLIA	nea	Habit: Small dwarfed plants. Leaves are round, bulged upwardly, rolled with lighter veins and of a somewhat darker green	xxx	xxx	xx	xx
OF	219	OBESIFRUTICOSA	of	Small and compact bushes with short main stem and up to 6 or 8 similar side shoots.	xxx	xxx	xxx	xx
OP	222	OPULENTIFLORA	op	Plants are short, strong and dwarfed. They are bushy due to many side shoots.	xxx	xxx	xx	xx
OB	223	OBSCURA	ob	Leaves are dark green with much anthocyanin. The leaves are small and rounded. They are often incurvated downwards.	xxx	xxx	xx	xx
OBT	225	OBTECTA	obt	Plants are bushy and strong. Leaves: Leaves are dense, rounded and bend downwards.	xxx	xxx	xx	xx
OLIV	231	OLIVACEA	oliv	Growth of young plants is somewhat reduced. Adult plants are smaller than normal. Young shoots have an olive green color. Leave stems are shortened. Leaves are yellowish gray green. They are more narrow than normal. Cotyledons and first pair of leaves have an olive green color. They are rolled inwardly.	xxx	xxx	xxx	xx
PARV	240	PARVIFLORA PARVULA	parv	Young plants with retarded growth. Plants are small and bushy. Leaves of a dark green. Seedlings of a darker green than normal and smaller.	xxx	xxx	xx	xx

PEV	248	PERVIRIDES	pev	The plants are smaller and darker green than normal. This can already be detected with seedlings. Leaves: Leaves are darker green than normal. They are more narrow than normal.	xxx	xxx	xx	xx
PHAN-AMA	250	PHANTASTICA AMBIGUA	phan-ama	Growth strongly retarded but less than phantastic antiqua. Leaves: Leaves are irregular and partly reduced to needle size. Leaves are often asymmetric. Many somatic back mutations. Depending on the time of the back mutation smaller or greater sectors arise, that are mostly heterozygous.	xxx	xxx	xx	xx
POR	262	PORRECTA	por	Very strong and bushy plants. Young plants have dark green leaves with much anthocyanin. Leaves are longer and broader than normal. First pair of leaves is more erect than normal.	xxx	xxx	xx	xx
PROD	264	PRODUCTA	prod	Side shoots are short and parallel to the main stem. Leaves: Young plants have green leaves with much red pigment. The leaves are more erect than normal. Seedlings: Seedlings are grey yellow.	xxx	xxx	xx	xx
PROL	265	PROLONGATA	prol	The internodes are long, also in the side shoots. Mutant is longer than normal. Leaves are dark green and shiny. The leaves are somewhat broader than normal. Lower leaves are bend stiffly downwards. The color of the cotyledons are lighter green. Hypocotyl: The hypocotyl is elongated.	xxx	xxx	xx	x
ROA	287	ROSULATA	roa	The mutant forms rosettes. Some plants later form shoots and inflorescences.	xxx	xxx	xx	xx
RUC	289	RUBELLICAULIS	ruc	Plants are very small. Leaves are narrow and pointed. Lower sides are with much anthocyanin. Cotyledones are light yellow green.	xxx	xxx	xx	x
RUS	290	RUBIDICAULIS	rus	Older plants have increasingly red colored stems and side shoots. They display a reddish brown up to dark red color, due to increased anthocyanin. Leaves are yellow green and more narrow than normal. Lower leaves are bleached.	xxx	xxx	xxx	xx
SA	292	SALICIFOLI A	sa	First pair of leaves stand upright and develop later than normal. All leaves are narrower than normal (0.5 to 6 width to length, normal is 2.2 to 6cm). The color of the leaves is darker than normal. Leaves are thicker and dangle.	xxx	xxx	xx	xx
SPA	302	SPADICEA	spa	Growth and development is normal. flower mutant	xxx	xxx	xx	xx

SPE	304	SPECIOSA	spe	Plants are more vigorous than the wild type. Leaves: Leaves are darker and broader than normal. Later they become rounded.	xxx	xxx	xxx	xx
SPLEN	306	SPLENDIDA	splen	Color is somewhat darker than normal. Growth somewhat retarded. First leaves are rounded or egg-shaped. Edges are folded upwards producing bulged spoons. Cotyledons are rounded.	xxx	xxx	xx	xx
SQUAM	307	SQUAMATA	squam	Growth is retarded. Plants stay smaller. Leaves: Leaves are dark green, narrow and shiny	xxx	xxx	xx	x
ST	311	STENE	st	Plants are strong with retarded growth. Leaves: Leaves are somewhat more narrow than normal. Older leaves are dark green, younger ones are lighter colored. The leaves are more dense than normal. Cotyledons are yellow grey green.	xxx	xxx	xx	xx
SUBA	317	SUBCRISPA	suba	Leaves are wavy, bend and tortuous-like Cincinnati but smaller. Cotyledons have an olive green color. They dangle somewhat.	xxx	xxx	xx	xx
SUB	318	SUBSISTENS	sub	Growth is much reduced. Leaves: Leaves are small, narrow and pointed. The leaves have a grey green color and much red pigment. Cotyledon s are small. Hypocotyl: Hypocotyl is longer than normal.	xxx	xxx	xx	xx
TA	325	TARDIUSCULA	ta	Strong and small bushes. Leaves: Leaves are smaller and more rounded and bulged than normal. Their colour is grey green.	xxx	xxx	xx	xx
TEN	326	TENEBRICA TENUIS	ten	Young plants show retarded growth. Leaves are darker green with much anthocyanin. Leaves are narrower than normal. The edges are very much folded upwards	xxx	xxx	xx	xx
TESS	328	TESSELATA	tess	Leaves are darker green than normal. The lower side has much anthocyanin. Leaves are somewhat more narrow than normal. Seedlings have longer stems than normal.	xxx	xxx	xxx	xx
TI	329	TINCTIFLOR A	ti	Low plants. Leaves: The younger leaves are lighter green. Older leaves have much anthocyanin. The leaves are narrow and densely inserted.	xxx	xxx	xx	xx
TON	330	TONSA	ton	Growth is retarded. Leaves: Leaves are small. The color is darker green. They are more narrow than normal. The edges are somewhat bend upwards. The leaf disks are somewhat bulged. Leaf edges and upper sides show much anthocyanin.	xxx	xxx	xx	xx
TU	334	TURRIFORMI S	tu	Growth of the plants is retarded. Leaves: Leaves are small, shiny, dark green and have much anthocyanin. The surface of the leaves is indented. Cotyledon s are rounded and slightly	xxx	xxx	xx	xx

				bulged.				
VEG	339	VEGATA	veg	The plants are somewhat smaller than normal and strong. Leaves: The leaves are broader and more rounded than normal. The colour is fresh green.	xxx	xxx	xx	xx
VER	341	VERSICOLOR NERVOSA	ver	Plants are small. Leaves: Leaves with white spotting. Leaves have much anthocyanin. Their size and form is irregular. Cotyledone s with white spotting.	xxx	xxx	xx	xx
VIRES	345	VIRESCENS	vires	Growth is retarded. Leaves: Young leaves have a lighter green color than normal. The leaves are smaller than normal and pointed. Later the leaves become darker and almost normal.	xxx	xxx	xx	xx
VIA	346	VIRGULTATA	via	Young plants are small yellow green with much anthocyanins. Older plants are low bushes with yellow green shoot tips. Cotyledone s are very tiny.	xxx	xxx	xxx	xx

Table S2 Phenotypic responses of *Antirrhinum majus* mutants to salinity stress (100mM and 200mM NaCl). The genotypes were characterized for their response to salinity stress after long-term exposure (21 days) of stressful agent by measurement of chlorophyll reduction (%), water reduction (%), height reduction (%) and shoot Na^+, K^+, Ca^{2+} and Mg^{2+}concentrations. In bold are highlighted the selected two contrasting snapdragon genotypes under salinity stress. Results are mean values of at least 5 biological replicates.

Locus name - (Gene)*	MAM ids	Chlorophyll reduction (%)		Water reduction (%)		Height reduction (%)		Sodium accumulation (g Kg^{-1} DW)			Potassium accumulation (g Kg^{-1} DW)		
		100 mM NaCl	200 mM NaCl	100 mM NaCl	200 mM NaCl	100 mM NaCl	200 mM NaCl	Ctrl	100 mM NaCl	200 mM NaCl	Ctrl	100 mM NaCl	200 mM NaCl
Aestiva (aes)	**7**	**96.1**	**98.9**	**72.2**	**74.6**	**35.1**	**38.6**	**2.98**	**17.76**	**33.00**	**28.17**	**21.13**	**33.31**
Globularis (glob)	144	53.9	75.5	33.7	63.1	23.3	41.1	3.97	35.60	37.43	27.89	39.86	23.56
Graminifolia (gram mut)	147	84.6	88.3	37.9	43.2	46.4	53.1	1.35	30.87	28.86	22.78	27.49	20.65
Luxurians (lux)	192	50.7	90.4	49.9	60.8	53.6	55.6	1.91	32.07	30.45	28.16	28.44	16.78
Obesifruticosa (of)	**219**	**33.9**	**40.5**	**32.2**	**46.5**	**28.4**	**59.5**	**1.44**	**41.38**	**42.90**	**25.79**	**29.88**	**18.28**
Opulentiflora (op)	222	75.4	83.9	32.1	57.7	14.1	69.9	2.55	35.60	37.74	30.19	29.52	21.84
Obtecta (obt)	225	65.5	67.4	30.7	50.0	50.7	54.7	1.45	23.60	22.07	21.29	18.83	17.30
Olivacea (oliv)	231	68.8	95.2	64.1	65.3	26.3	41.4	1.55	21.21	36.19	23.25	18.03	12.98
Speciosa (spe)	304	74.3	81.6	31.1	55.5	22.2	51.7	2.59	45.42	36.26	24.45	27.47	19.29
Subsistens (sub)	318	69.0	73.8	43.9	65.8	35.8	39.7	1.66	42.32	49.72	32.26	30.67	18.91
Tesselata (tess)	328	69.7	73.3	39.9	67.1	38.5	40.4	1.85	40.07	47.10	19.6	30.46	20.96
Virgultata (via)	346	52.2	67.7	31.7	53.4	24.4	50.2	4.06	31.78	40.83	20.12	23.56	20.29
Rubidicaulis (rus)	290	73.5	79.8	40.4	55.0	29.0	42.0	7.4	40.76	40.17	24.55	24.16	20.03

Supplementary Material

Click here to download Supplementary Material: Supplementary Tables S3-S11.xlsx